Study of creep and stress relaxation behaviour of PLA-PCL for development of a biodegradable ligament device

Cátia Sofia Neves Martins

Relatório da Dissertação do MIEM

Orientador: Prof. Rui Miranda Guedes

Supervisor: Prof. António Torres Marques

Faculdade de Engenharia da Universidade do Porto

Mestrado Integrado em Engenharia Mecânica

Fevereiro 2014

À minha família e amigos

Abstract

Injuries to tissues such as/like ligaments and tendons are very common, especially in the case of high competition athletes. The current gold standard technique for ligament replacement is auto grafting. However, in the initial phase of rehabilitation, mechanical properties of the graft degrade due to synovial liquid aggression. Hence, the bounding resistance of the suture is problematic during the tissue's recovery, implying reduction of mobility for several months.

In the scope of this project, the biodegradable composite material, PLA-PCL, was studied as a possible solution for ligament reinforcement. The main focus was to analyse the creep and stress relaxation behaviour of PLA-PCL fibres and investigate the performance of a simple linear viscoelastic model, the Burgers (or four element) model, describing both these behaviours. Thus, tensile, creep and stress relaxation tests were performed both in dry and saturated specimens. Multiple levels of creep and relaxation were defined in order to understand the stress/strain-dependence of creep/stress relaxation rate behaviour. Finally, the modelling of creep testing data was made based on the model's equation to obtain the Burgers parameters (R_1, R_2, η_1, η_2). With these values and imposing the experimental strain in the Burgers equation, it is possible to obtain a prediction of the stress relaxation behaviour of PLA-PCL fibres based on their creep experiments.

The results of mechanical tests performed proved that PLA-PCL displays, similarly to the natural ligament tissue, a nonlinear ligament tissue, based on the shape of the stress-strain curve. Creep and relaxation data suggests the rate of creep/stress relaxation decreases with increasing stress/strain. The linear viscoelastic approach seems to be valid up to a certain stress level which is referred to as the linear viscoelastic threshold. However, above this stress level the response of PLA-PCL becomes nonlinear, so more complex and nonlinear models should be considered in order to achieve better modelling results.

Keywords: polylactide (PLA), ligament replacement, viscoelastic behaviour, creep, stress relaxation, Burgers model

Estudo do comportamento à fluência e à relaxação de tensões do PLA-PCL para desenvolvimento de um dispositivo ligamentar biodegradável

Resumo

Lesões em ligamentos e tendões são muito frequentes, especialmente em praticantes de desportos como basquetebol, futebol, esqui e futebol americano. Atualmente, as técnicas de autoenxerto são a solução mais adotada nas cirurgias de substituição destes tecidos. Contudo, numa fase inicial do período de recuperação, as propriedades mecânicas do enxerto são afetadas devido à agressão do líquido sinovial. Por este motivo, durante a regeneração do novo tecido a resistência da sutura é problemática, tendo como consequência a redução da mobilidade do paciente durante vários meses.

No âmbito deste projeto, o material compósito biodegradável PLA-PCL, foi estudado como uma possível solução como reforço ligamentar. O objetivo principal foi analisar o comportamento à fluência e relaxação de tensões de fibras de PLA-PCL e investigar o desempenho de um modelo linear viscoelástico relativamente simples, o modelo de Burgers (ou modelo de quatro elementos), na descrição destes comportamentos. Assim, foram realizados ensaios de tração, de fluência e de relaxação de tensões a fibras secas e a fibras saturadas. Foram definidos vários níveis de fluência e relaxação de forma a perceber qual a relação das taxas de fluência/relaxação de tensões em função da tensão/deformação. Finamente, foi realizada a modelação dos resultados de fluência com base na equação do modelo e calculados os parâmetros de Burgers (R_1, R_2, η_1, η_2). Com estes valores e impondo a deformação experimental na equação de Burgers, é possível obter uma previsão do comportamento à relaxação de tensões das fibras de PLA-PCL com base nos ensaios de fluência.

Os resultados dos ensaios mecânicos provaram que o compósito PLA-PCL tem um comportamento não linear viscoelástico semelhante ao do ligamento natural que é evidenciado no formato da curva tensão-deformação. Os dados dos ensaios de fluência e relaxação sugerem que a taxa de fluência/relaxação de tensões diminui com o aumento da tensão/deformação. A abordagem viscoelástica linear parece ser válida até um determinado nível de tensão conhecido como o limiar da região linear viscoelástica. No entanto, acima deste nível de tensão, a resposta do compósito polimérico torna-se não linear pelo que é preferível uma análise com base em modelos mais complexos e não lineares a fim de alcançar melhores resultados na modelação dos dados experimentais.

Agradecimentos

Ao pensar em todo o percurso percorrido até concluir esta tese, não posso deixar de pensar igualmente nas pessoas que foram importantes ao longo destes meses de trabalho. Por essa razão, desejo expressar os meus sinceros agradecimentos:

Ao Professor Doutor António Torres Marques, meu supervisor, por ter aceitado orientar a minha dissertação numa área do meu interesse, pela sugestão de um tema tão interessante e por toda a disponibilidade demonstrada.

Ao Professor Doutor Rui Miranda Guedes, meu orientador, pelo acompanhamento do trabalho, pela disponibilidade e generosidade, e por toda a ajuda prestada ao longo destes meses de trabalho.

À Engenheira Viviana Correia Pinto, Laboratório de Mecânica Experimental (LOME), pela disponibilidade e generosidade demonstradas no acompanhamento de todo o trabalho experimental realizado.

Ao meu namorado, António, o meu grande apoio neste percurso, pelo carinho, paciência e compreensão reveladas em momentos mais complicados, bem como pelas inúmeras trocas de impressões, correções e comentários ao meu trabalho, estimulando-me a crescer científica e pessoalmente.

Aos meus pais e irmão, por todo o carinho, apoio, paciência e amizade demonstrados ao longo destes meses, mesmo quando eu não facilitava.

Aos meus amigos, nomeadamente, Susana, Joana, Pedro (trapa), Rafael, Daniel, Romina e Bruno pela amizade e por todos os bons momentos passados em conjunto.

Contents

Figures Index

Tables Index

1 Introduction

"Ligaments and tendons are load-bearing, soft fibrous tissues that connect bones within joints" [1]. Ligaments have both ends inserted into bones and connect them to each other; whereas tendons have only one insertion because the other end is joined with the muscle and connect skeletal muscles to bones [2, 3]. This is the main difference between these two dense connective tissues.

Injuries to tendons and ligaments are very common, with over 800,000 people seeking medical attention each year [4, 5]. It has been estimated that the incidence of knee ligament injuries could be at 2/1000 people per year in the general population and a much higher rate for those involved in sports activities. Frequently, surgery is required, but the outcomes are variable. However, the recent procedures of accelerated post-surgical rehabilitation allow a faster return to functional activities, like work or athletic competition, with 4-6 months postoperatively, rather than 9-12 months [4, 6]. The anterior cruciate ligament (ACL) is a ligament of the knee that controls motion by connecting the femur to the tibia and stabilizing the joint [7]. Along with medial collateral ligament (MCL), the ACL is one of the most important and studied ligaments and also the one that is ruptured the most [1]. According to several authors, over 150,000 ACL surgeries are performed annually in the United States [4, 5, 8, 9].

Although tissues like ligaments and tendons sustain excessive mechanical loads, they have a poor regeneration capacity with their low cell density and low nutrient and oxygen requirements [10]. Mature tendons/ligaments are poorly vascularised and its nutrition relies on synovial fluid diffusion rather than vascular perfusion [11]. The ACL, for example, is surrounded by the synovial fluid which prevents clot formation, thereby impeding the healing. Additionally, the high extracellular matrix (ECM) density and organization along with the presence of few blood vessels further complicates self-healing.

Current surgical reparative techniques for ligament/tendons injuries rely on tissue replacement with auto- or allograft [12]. An ACL reconstruction surgical auto grafting involves using part of the patient own patellar tendon, hamstring or quadriceps to replace the ruptured one. "Alternatively, allograft can be used where the donor tendon is taken from a cadaver" [9]. Both possess good initial mechanical strength and compatibility, promoting cell proliferation and incorporation of the graft on the new tissue formation [4, 5, 10] but each treatment has pros and cons associated.

The current auto grafting techniques for ligament repair remain the gold standard, having high revascularization and remodelling capacities. However, this treatment causes

donor site morbidity which is associated with pain and a recovery period for the donor tissue site. Although 75-90% of patients treated with auto grafts have good or excellent long term success rates, there are a substantial number of patients who have unsatisfactory results which could be attributed to graft failure, being long-term rupture or excessive laxity the main mechanical causes. Comparatively, the allograft solution have disadvantages like donor scarcity, risk of disease transmission, infection, allergic reactions in addition to their lower early cellularity and less revascularization or tissue rejection but the risks associated with auto grafts are excluded (such as donor site morbidity) [4, 5, 9, 10]. "A more ideal solution would be to fully restore the tendon or ligament tissue to its pre-injured state" [12].

This is the promise of tissue engineering, a method which combines knowledge from material science, engineering, molecular biology and medicine, being an ever expanding field, aiming to develop biological substitutes to restore, maintain or improve tissue function [9, 11]. Conceptually, this field's goal is to incorporate specific cell types into a biodegradable scaffold which when implanted will gradually regenerate into a tissue that closely resembles the original one and restores its functionality [12]. "The choice of appropriate cells and a suitable scaffold are crucial to achieve success in this approach" [13]. Tissue engineering strategy involves using biodegradable and biocompatible biomaterials with adequate structural and mechanical properties to mimic the organization of the native tissue, along with cells isolated from the healthy proportion of the patients own ligament, or other alternative cell sources such as stem cells, and growth factors to regulate its function [10].

Tendons and ligaments are highly organised 3-dimensional (3D) structures [11]. "A common approach in tissue engineering involves a three-dimensional porous biodegradable scaffold loaded with specific living cells and/or tissue-inducing factors to launch tissue regeneration or replacement in a natural way" [3]. The degradation rate of the scaffold experiencing biodegradation *in vivo* must be compatible with the growth rate of biological tissue. So, by the time the injury site is healed, the scaffold should be totally degraded. For medical applications, scaffolds must have specific characteristics because they are exposed to numerous biological and mechanical factors when implanted into the body. Besides being biocompatible, the scaffold material should not elicit inflammatory response or demonstrate immunogenicity or cytotoxicity [11].

"From the clinical point of view, the main advantages offered by the use of tissue engineered ligament could be listed as minimal patient morbidity, simpler surgical technique, reliable fixation methods, rapid return to pre-injury functions, minimal risk for infection or disease transmission, biodegradation at a rate that provides adequate mechanical stability, and supporting host tissue ingrowths'" [10].

Synthetic and natural polymers have been studied in tissue engineering as viable solutions for ligament replacements. Polydioxanone (PDO), polycaprolactone (PCL), polylactic acid (PLA), poly-l-lactide (PLLA), polylactic-*co*-glycolic acid (PLGA), polylactic-co-glycolic acid (PLAGA), polyglycolic acid (PGA) are some examples of these synthetic materials, whereas silk, gelatin, collagen, elastin and fibrinogen are natural polymers [9, 11, 14].

Thus, to achieve success with the tissue engineering approach a scaffold must be biocompatible and promote tissue in growth, display similar mechanical behaviour when swelled to saturation (shape of the stress–strain and stress relaxation response), be creep

resistant and degrade at a rate that does not cause stress shielding or rupture of the new tissue [3, 4].

The current solutions for soft tissues are based on materials susceptible to visco-elasto-plastic behaviour, such as polymers, which may lead to failure of the device. “In many applications, the materials are submitted to large deformations, above the elastic limit, in dynamic or static loading conditions, and therefore they will progressively accumulate damage due to fatigue or creep” [15]. Biodegradable devices can fail in long term due laxity or by sudden failure and, in the case of polymers, creep and fatigue interactions occur at low temperature and these two phenomena are coupled [4, 15].

According to Spathis et al. [16], “prediction of the deformation and long-term strength of polymeric materials has extensively been studied independently as a visco-elasto–plastic behaviour.” This is due to the mechanical behaviour of polymers, governed by both rheological (time-dependent) effects and plastic deformation [16].

In this work, the focus is given to the study of the creep and stress relaxation behaviour of the biodegradable composite PLA-PCL, to investigate its suitability as part of a ligament tissue reinforcement. Later, a viscoelastic model, the Burgers or four element model, is used to describe the experimental data.

2 Literature review

This literature review is divided in three different sections. The first one gives an overview about the natural ligament and tendon tissues, including a subsection about the anterior cruciate ligament. In the second one, about biomaterials, it is presented what kind of work has been done on the tissue engineering field for the replacement of tendons/ligaments. Due to the subject of this thesis, the emphasis is given to studies about PLA and its composites that have attracted the interest of researchers. The last section is dedicated to the viscoelastic models and the Burgers model is presented, which will later be used for modelling the tests data.

2.1 Natural tendon/ligament tissue: An overview

All connective tissues show a complex mechanical behaviour that is directly related to their hierarchical structure and to their specific macromolecular components. As a result of decades of mechanical investigations at higher hierarchical levels, that is whole tissues and collagen fibres, it is well known that collagen-rich tissues present nonlinear viscoelastic behaviour, as conclusively proved from a larger number of creep and relaxation tests that have been performed on both tendons and ligaments. This viscoelastic behaviour can be observed when the tissue is subjected to a cyclic loading. The stress-strain relationship in the loading curve is usually not coincident with the unloading curve, but instead form a hysteresis loop representing internal energy dissipation (or non-recoverable energy) [2, 17-19].

Many viscoelastic constitutive formulations have been proposed to model biological soft tissues such as the quasilinear viscoelasticity (QLV) theory, proposed by Fung in 1993, the nonlinear superposition or the nonlinear theory of Schapery [20]. Despite its great contribution to biological tissue modelling, the QLV models have various limitations: they cannot account for creep and relaxation rate dependency tissues and they cannot usually interrelate creep and relaxation. For tissues like ligaments, that show a rate dependency a high stress and strain levels, the QLV models are not successful at predicting their creep behaviour based on relaxation experiments or vice versa. “These findings suggest that viscoelastic phenomena in ligaments occur through fundamentally different mechanisms and time dependent behaviour of the tissue cannot be successfully captured by this theory” [21].

The viscoelastic behaviour of ligaments and tendons has important clinical significance as they help to prevent fatigue failure. During daily activities such as walking or jogging,

cyclic stress relaxation occurs in which the peak stress in the tissue substance decreases with each cycle [19]. In an *in vivo* relax situation the ligament tissue is pre-tensed. Hence, they work as a spring, enabling the muscle to distend after a contraction and preventing its buckling.

2.1.1 Tendons and ligaments

"Tendons and ligaments are dense and regularly arranged connective tissues made of fibres that induce or guide joint movement" [4]. They are comprised of a cellular component, consisting mainly of fibroblasts, and an extracellular matrix (ECM) component composed of collagen, proteoglycans, tenascin-C, and small amounts of other proteins (see Table 1). The fibroblasts (located within in the ECM) are responsible for producing the ECM components to maintain and repair the tissue, and after an injury these cells mobilize, migrating to the wounded tissue to aid in repairing [4, 9]. An illustration of these tissues' structure can be seen in Figure 1.

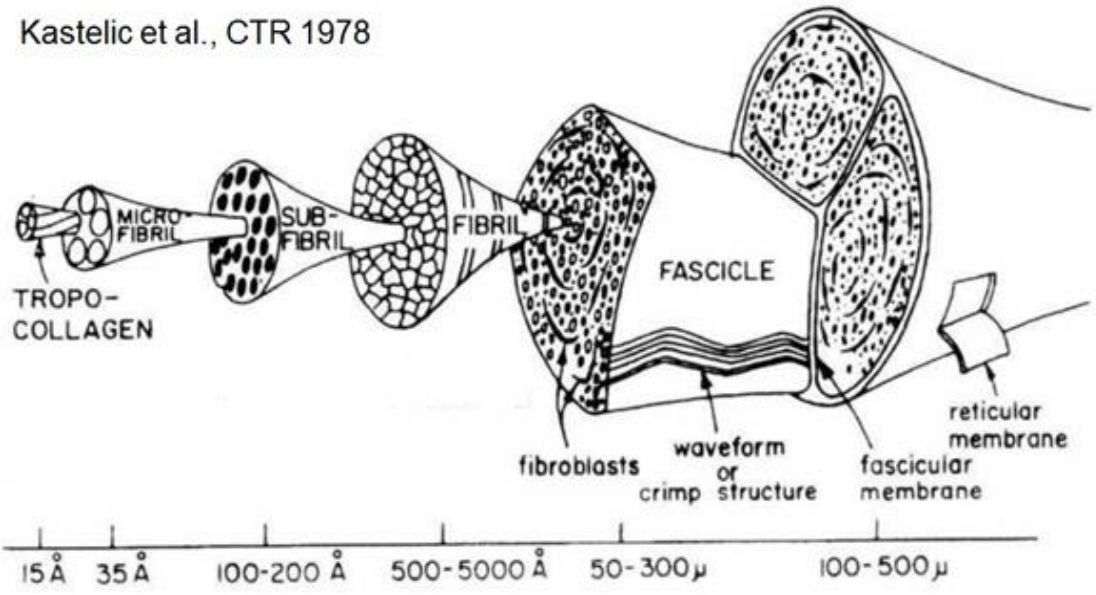

Figure 1 Tendon/Ligament Structure

As previously mentioned, the largest component of tendon and ligament tissue's ECM is collagen (primarily types I and III). The ability of collagen to provide strength is an important characteristic that is directly related to the structure of the molecule and its capacity to form cross-links. While collagen provide tensile strength, tenascin-c, a type of protein found in ligament ECM, regulates the tissues response to mechanical loading [4, 9].

Another important component of the tendon and ligament ECM are proteoglycans, due to their contribution to viscoelastic behaviour and to other mechanical properties of the tissue. The most abundant proteoglycan in tendon tissue is decorin, a constituent that inhibits formation of large collagen fibrils allowing the tissue to adapt and compensate for tensile

strength. Aggrecan, another proteoglycan, is found abundantly in areas where the tissue is subject to compressive forces [4].

"The individual collagen fibrils are randomly orientated, but as they aggregate into fibres they gain a more parallel orientation with the longitudinal axis of the ligament, giving the tissue a crimping pattern (wavy appearance)" [9].

Table 1 Major constituents of wet ligaments [9]

Tissue Type	**Collagen type I [%]**	**Other collagens (III, V, VI) [%]**	**Elastin [%]**	**Fibronectin and other glycoproteins [%]**	**Proteoglycans [%]**	**Water [%]**
Ligament (general)	20	3-5	1-2	1-2	< 1	70

Due to the arrangement of their components, ligaments display 3 stages of behaviour when tensile loaded (see Figure 2). First, there is an area where the ligament exhibits a low stiffness region known as the toe region. When a force is applied to the tissue, it is transferred to the collagen fibrils, resulting in lateral contraction of fibrils and straightening of the crimp pattern. Following this, it displays an increase in stiffness, corresponding to the linear region and since the collagen fibres are straightened, this corresponds to collagen stiffness. The last area, the yield and failure region, exhibits a decrease in slope and represents the defibrillation of the ligament [5].

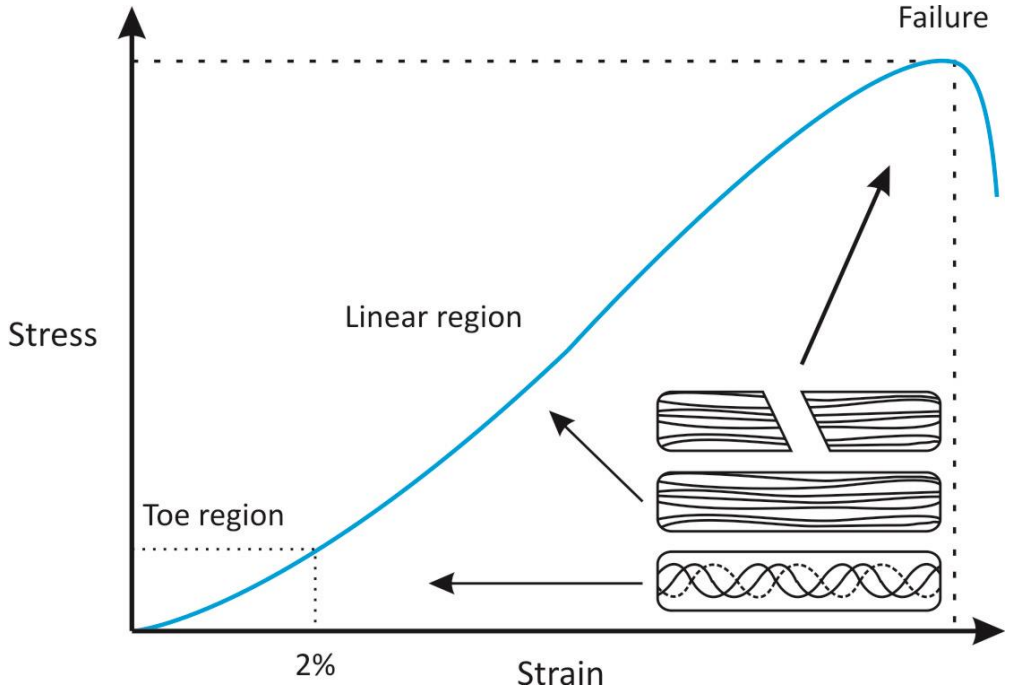

Figure 2 Stress-strain behaviour of a ligament [22]

2.1.2 Anterior Cruciate Ligament (ACL)

The anterior cruciate ligament is one of the four major ligaments of the human knee, which functions as a joint stabilizer (see Figure 3). This ligament originates from deep within the notch (compartment) of the distal femur connecting it to the tibia. The way it is attached to other tissues allows it to resist anterior translation to de tibia in relation to the femur. Mostly in sports activities, lateral rotational movements are what cause the ACL to strain or tear [4, 9].

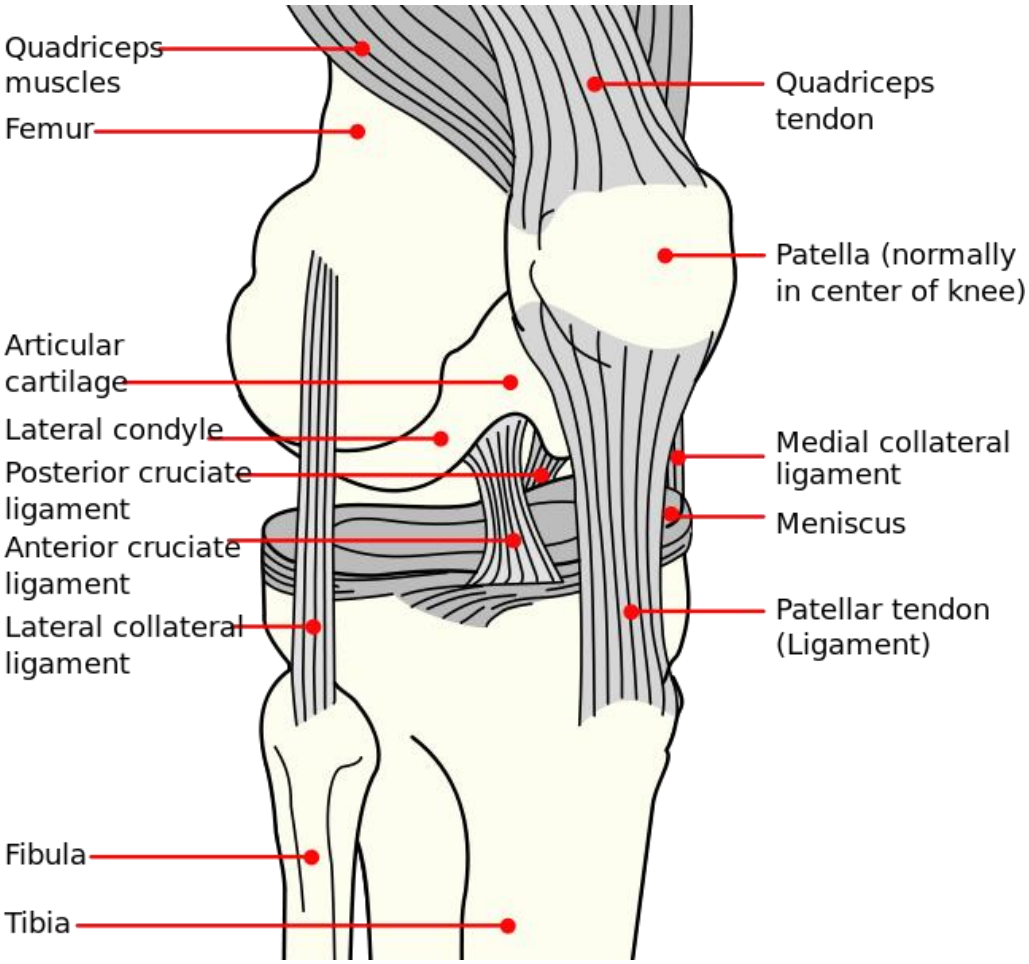

Figure 3 Anatomical view of knee joint[1]

It is well known that ACL has limited capacity for healing after its injury. Unlike extra-articular ligaments, there are several factors that limit the tissue recovery. For example, the thin synovium that surrounds this ligament, which has been shown to play an important role in providing a vascular supply to the relatively avascular ACL as well as to protect it from the harsh synovial fluid, does not regenerate until 1 to 2 months following an injury [19]. Hence the need for a device as temporary replacements for the tissue while it regenerates.

Similar to what was done in section 2.1.1, in the Table 2 are listed the constituents of the anterior cruciate ligament.

[1] http://en.wikipedia.org/wiki/File:Knee_diagram.svg. Access: February 5, 2014

Table 2 The collagen content of the ACL in dry tissue (*adapted from* [9])

Tissue Type	Collagen type I [%]	Collagen type III [%]	Collagen type V [%]	Ratio of collagen I:III	Reference
ACL	70-80	8-10	10-12	9:1	[4, 9]

The André Vieira's doctoral thesis [4] has an excellent collection of data about morphological and biomechanical properties of this soft tissue and it is presented here in Table 3.

Table 3 Morphologic and biomechanical properties of the ACL [4]

Properties	Values	References
Length	**27 – 32 mm** **31 – 38 mm** *male:* **26.9– 32.3 mm** *female:* **24.1 – 29.9 mm**	(Freeman et al., 2006) (Karmani and Ember, 2003) (Chandrashekar et al., 2006)
Minimum Area	*male:* **54 – 91.8 mm^2** *female:* **41.6 – 73 mm^2**	(Chandrashekar et al., 2006)
Volume	*male:* **2016 – 3428 mm^3** *female:* **1466 – 2526 mm^3**	(Chandrashekar et al., 2006)
Toe Region limit	**2.0% - 4.8% strain** **1.5% - 4.0% strain**	(Chen and Black, 1980) (Karmani and Ember, 2003)
Rupture or Tearing limit	**7% to 16%** **10% to 15%**	(Chen and Black, 1980) (Karmani and Ember, 2003)
Load at normal physical activity	**67 - 700N**	(Chen and Black, 1980; Black, 1992; Black, 1998)
Elongation at Rupture	*male:* **6.8 – 11 mm** *female:* **4.9 – 10 mm**	(Chandrashekar et al., 2006)
Strain at Rupture	*male:* **24% - 36%** *female:* **19% - 35%**	(Chandrashekar et al., 2006)
Maximum Load	*male:* **1119 - 2517N** *female:* **739 - 1793N** **1725 - 2195N** **2000 - 2300N**	(Chandrashekar et al., 2006) (Karmani and Ember, 2003) (Woo et al., 1991)
Maximum Stress	*male:* **16.3–36.4 MPa** *female:* **13.7–31.5 MPa**	(Chandrashekar et al., 2006)
Linear Stiffness	*male:* **219–397 N/mm** *female:* **111–287 N/mm** **210 – 270 N/mm**	(Chandrashekar et al., 2006) (Woo et al., 1991)
Young Modulus	*male:* **93 - 163 MPa** *female:* **49 - 149 MPa**	(Chandrashekar et al., 2006)

2.2 Biomaterials

2.2.1 The beginning: nondegradable synthetic grafts

In the 1970s, the interest for synthetic grafts led to their introduction as substitutes for biological human tissue. The increased appeal of these supports resulted in the commercialization of products such as Proplast® ligaments, made of Teflon® and carbon and Polyflex®, made of polypropylene. However, results were not satisfactory since both methods had to be withdrawn from the market due to their high rupture rate and inflammatory reaction in the surrounding tissues. Furthermore, experimental studies conducted on these materials showed their unsuitable mechanical properties [23].

In 1977, an artificial ligament made of carbon fibre was developed and after being initially employed for tendon sutures, its use was then extended to ligament reconstruction in the knee and other joints. In 1981, the first carbon-fibre reinforced substitute for ACL was implanted with an arthroscopic procedure. "However, after preliminary encouraging results, serious sequels were observed during clinical application. It has been demonstrated that the poor resistance to torsion forces caused an early rupture of the fibres leading to carbon deposits in the liver and inflammatory synovitis in the knee joint" [23]. Others nondegradable synthetic materials that have also been used for anterior cruciate ligament repair include polyethylene terephthalate (Leeds-Keio® ligament), polytetrafluoroethylene (Gore-Tex®), and polypropylene (Kennedy Ligament Augmentation Device). These synthetic ligament replacements have been conditionally approved by the FDA for testing and augmentation but are not recommended for primary ACL repair [7, 9, 24].

Nondegradable polymers like DACRON®, polytetrafluoroethylene, polyester, polypropylene or carbon fibres have shown unsuccessful results in the long term. Although most of these synthetic materials have superior mechanical characteristics compared to biological scaffolds, they don't approximate the material properties of tendon or ligament, resulting in stress shielding of new tissue formed, long-term rupture by fatigue, excessive laxity due to material creep, fragmentation or wear debris, ultimately lead to implant failure. For all these reasons, some of these materials were completely abandoned [3-5, 25].

Table 4 Advantages and disadvantages of auto, allo and synthetic grafts (*adapted from* [9])

	Auto graft	**Allograft**	**Synthetic graft**
Advantages	No rejection, disease transmission or donor scarcity.	No donor site morbidity.	No tissue disease transmission, donor site morbidity or scarcity.
Disadvantages	Donor site morbidity; Limited bone integration; Patellar fracture; Quadriceps weakness; Mismatch in different tissue properties causing mechanical failure, creeping and fatigue; Recurring injury.	Donor scarcity; Limited bone integration; Tissue rejection; Mismatch in different tissue properties causing mechanical failure, creeping and fatigue; Recurring injury.	Limited bone integration (weak graft-host tissue interface); Mismatch in different tissue properties causing mechanical failure, creeping and fatigue; Poor long-term stability; Recurring injury.

2.2.2 Biodegradable synthetic polymers

The search for more compatible materials with the human body led to consider bio-absorbable polymers (BAPs) as an option for ligament regeneration. BAPs' thermal degradation is very fast in presence of moisture because these polymers are moisture and heat sensitive. Biodegradation mainly depends on type of material, molar mass, percentage of crystallinity, type of environment (enzymatic concentration, external stress) and material moulding history (internal stress) [26].

Bioabsorbable implants have three main disadvantages: lower strength, higher cost, and, in some cases, undesired biological response. However, many studies have shown that biodegradable devices can provide the necessary initial strength for orthopaedic applications as long as the application is chosen with care, and other studies have shown that the strength reduction during degradation is slow enough to allow tissue healing. Furthermore, the high initial cost of the implant can be offset when one considers the added expense for a second surgery to remove a nondegradable device [27]. Thus, "the growing emphasis on the use of biodegradable materials is due to the fact that these materials do not elicit a permanent foreign body reaction, as they are gradually reabsorbed and replaced by natural tissue" [28].

Aliphatic polyesters are an important class of biodegradable polymers because the products of the hydrolysis reaction are naturally metabolized by the human body. Polylactide (PLA), polyglycolic acid (PGA), polycaprolactone (PCL) and polyhydroxyalkanoates (PHA's) are some examples of these materials. A variety of biomedical applications and devices have been produced since 1970's from synthetic biodegradable PLA, PGA, and copolymers of these polymers [4, 8, 9].

PLA is a hydrophobic polymer and PGA is a hydrophilic material, which presents a high degradation rate, and the combination of these two polymers is usually employed to tune

degradation rate [4]. The main mechanical properties, Young modulus, tensile strength and elongation, of some bioabsorbable polymers are listed on Table 5.

Table 5 Mechanical properties of some BAP's

BAP	*Young Modulus (MPa)*	*Tensile Strength (MPa)*	*Elongation (%)*	*Reference*
PLA	350-3500	21-60	2.5-6	[4]
	350	21	2.5	[29]
PLLA	2700-4140	15.5-150	3-10	[4]
	2700	15.5	3	[29]
PDLLA	1000-3450	26-50	2-11.4	[4]
	1000	27.6	2	[29]
PGA	6000-7000	37-100	1.5-20	[4]
	6000	60	1.5	[29]
PCL	210-440	20.7-42	300-1000	[4]
	210	20.7	300	[29]

"Polymers failure, over a range of loading conditions and frequencies, was found to occur at a critical level of cumulative strain" [4]. Unlike the natural living tissue that is able to remodel and self-repair injury, synthetic materials will always accumulate unrecoverable damage. Thus, when using a biodegradable polymer, the cells are expected to attach to the material surface, proliferate and produce the ECM that will gradually replace the mechanical functions of the device. This defines the general concept of regenerative reconstruction devices [4].

Besides mechanical time dependent damage, common to all polymers, one must consider damage due to hydrolysis [4].

a) PLA (polylactide)

PLA can be obtained from natural sources like starch. There are two main different PLA types: poly (L-lactide) PLLA and poly (D-lactide) PDLA. The latter has a much higher degradation rate than the former. [4, 30, 31].

The degradation rate of this polymer depends on its crystallinity degree, material shape, molecular weight and also on the site of implantation. Polylactide has a very slow degradation rate and, according to Vieira et al., it degrades completely into lactic acid within a period ranging from 10 months to 4 years, depending upon all the mentioned parameters [4].

However, other studies report that high molecular-weight PLA can take between 2 and 5 years for total *in vivo* reabsorption [30].

Its mechanical properties make PLA an ideal candidate for load-bearing applications, such as fixation devices and sutures, and it has also been tested as a replacement solution for tendons and ligaments due to the high strength of its fibres. On the other hand, this polyester has as disadvantages its brittleness and poor thermal stability. Since high molecular weight PLAs have, in general, better mechanical properties, many companies commercialize PLA with various ratios of D or L lactide. In the Table 6 are listed the trade names and suppliers of different grades of PLA [30, 31].

Table 6 Trade names and suppliers of PLA (*adapted from* [22])

Trade names	Company	Country
NatureWorks®	Cargill Dow	USA
Galacid®	Galactic	Belgium
Lacea®	Mitsui Chem.	Japan
Lacty®	Shimadzu	Japan
Heplon®	Chronopol	USA
CPLA®	Dainippon Ink Chem.	Japan
Eco plastic®	Toyota	Japan
Treofan®	Treofan	Netherlands
PDLA®	Purac	Netherlands
Ecoloju®	Mitsubishi	Japans
Biomer® L	Biomer	Germany

b) PLLA (poly-L-lactic acid)

PLLA has been researched for use in tissue-engineering applications. Unlike auto grafts, there is no limit to the supply of these polymeric matrices, the risk of disease transmission is minimal and they can be easily sterilized without significant alteration of mechanical properties. In a degradation study, PLLA fibres displayed very little change in mechanical properties over an 8-week period, on average [7].

In 1993, Laitinen et al. tested the mechanical properties of braided PLLA implants *in vitro* and after subcutaneous implantation in rabbits. These implants have shown better mechanical strength and a slower degradation rate than PDO and PGA, which would be advantageous for reconstruction of the anterior cruciate ligament [32].

Cooper and his colleagues, in their ligament regeneration studies, have developed a tissue-engineered solution based on a cell seeded, degradable, three-dimensional braided PLLA scaffold. The design parameters of the braid and the composition of the braid fibres promote ACL cell attachment and proliferation. When submerged in phosphate-buffered saline (PBS) for up to 12 weeks, the mass of the scaffold did not decrease and the average molecular weight of the scaffold showed a linear decrease over the degradation period. There was also no significant decrease in mechanical properties over a 12-week degradation period [28, 33].

To achieve better results, Cooper et al. decided to add a growth factor to the PLLA scaffolds, the fibronectin (Fn). The pre-coated PLLA-Fn scaffold has been shown to improve cell attachment efficiency, cell proliferation, and long-term matrix production by ACL cells on the 3-D braided matrix [7].

The results of a more recent research study, carried out by Surrao and his colleagues, suggested that PLLA on its own would not be suitable as a scaffolding material for ligament tissue engineering. Alternatively, copolymerizing L-lactide with D,L-lactide or glycolide may be an effective way of improving its properties for this purpose [1].

c) PLGA or PLAGA (polylactide-co-glycolide)

Synthetic poly (α-hydroxy acids) like PGA, PLA and their copolymer, PLGA could be used to fabricate mechanically strong and biodegradable porous scaffolds, possessing good biological compatibility, to suit the purpose. These polymers offer several advantages over other materials with respect to design, flexibility, controllable porosity and degradation rate. PLGA has been used widely as surgical sutures and it can be fabricated into 3-D scaffolds of variable structure and porosity, having a wide range of mechanical and degradation properties. Results of experimental researches have demonstrated that ACL cells and BMSCs adhere to and proliferate better on PLGA than on other materials such as PCL, PLA, or PCL-PLA copolymers [3].

In 2005, Cooper and his colleagues tried to engineer functional anterior cruciate ligament scaffolds based on three-dimensional fibrous hierarchical designs, utilizing novel braiding techniques which permit, among other things, controlled fabrication of substrates with desired mechanical properties and geometry, by mimicking the collagen fibre matrix of the natural tissue. For this purpose, PLAGA fibres were chosen for study as part of a tissue-engineered scaffold [28].

Mechanical properties such as elastic modulus and tensile strength of two types of braided ligament scaffolds (rectangular and circular) were compared, in order to select an optimal braiding geometry for a tissue-engineered ACL scaffold. The stress–strain profiles looked similar to what would be expected of natural ligament tissue. When the same number of yarns was used for the rectangular and circular braids, the circular braid geometry showed a significant increase in maximum tensile load, being able to withstand tensile loads of 907 N (St. Dev.±132 N), which was greater than the level for normal human physical activity that is

estimated to range between 67 and 700 N. The biocompatibility of the scaffold was confirmed by the results, as both cell types attached and proliferated on the scaffold [28].

Lu et al. [33] decided to explore the utilization of fibronectin (Fn) in ACL tissue-engineering scaffolds. Therefore, three compositions of poly-α-hydroxyester fibres with varying rates of degradation were considered, namely PGA, PLAGA, and PLLA. The attachment and growth of ACL cells on these three types of polymers were examined and it was hypothesized that cellular response will be dependent on polymer composition, and the Fn coated polymeric surfaces would promote cell adhesion in this tissue-engineered system.

At day 14, cells grown on braided scaffolds pre-coated with Fn continue to elaborate larger amount of matrix compared to PLAGA or PLLA scaffolds without Fn. The difference between the surface-modified scaffold and untreated surface became more pronounced at this time point. The circular 3x8 braided scaffold of PLAGA measured a maximum load of 215±23 N and an ultimate tensile strength of 117±12 MPa [33].

One year later, Sahoo et al. developed a novel, biodegradable nano-microfibrous polymer scaffold by electro spinning PLGA nanofibres onto a knitted PLGA scaffold in order to provide a large biomimetic surface for cell attachment. Although the results of the mechanical tests have shown that, for stronger tissues like tendon and ligament, the scaffold alone does not provide sufficient strength, this novel nano-microfibrous scaffold remains an important achievement. While knitted microfibers provide the mechanical integrity, the nanofibres, randomly spread over the surface and between the loops of the knitted scaffold, increase the surface area and reduce the pore size of the scaffold [3, 34].

d) PLA-PCL

Polycaprolactone (PCL), suitable for long-term use in implants, presents a slower degradation rate than those of PLLA and PGA. Since this polyester is very ductile and presents low stiffness, the PLA-PCL blend improves the mechanical properties of pure PLA. On the other hand, the degradation products of PLA are known to reduce local pH, accelerate degradation and induce inflammatory reactions which can be minimized by the new material [4, 31, 35]

In his work, André Vieira [4] studied the following composition of the composite PLA-PCL [90:10]. Despite static test results and degradation rate point to PLA-PCL as a good option for ligament augmentation devices, in terms of stiffness and strength evolution, this material alone is prone to creep, showing a very strong time-dependency, which induces laxity that compromise the stability of the knee. This conclusion, extended to other biodegradable polymers, may justify many unsuccessful synthetic solutions for scaffolds.

When dynamic analysis was performed, the conclusions were that the material presented strong viscoelastic/viscoplastic behaviour that causes premature failure or excessive laxity of the biodegradable medical device, even for very low load levels far below the static strength. The PLA-PCL composite has higher rate dependency compared to other thermoplastics so it accumulates mechanical damage, in the form of plastic deformation, up to

a critical level when it breaks. The conclusion was that failure happens due to laxity, long before rupture occurs [4].

However, a plausible solution to fulfil maximum laxity requirements could be reinforcing the PLA-PCL with a material unsusceptible to creep, such as Phosphate Bio-Glass (PBG) which is a biodegradable glass that can be combined with biodegradable polymers. These materials are not susceptible to viscoplastic strain accumulation [4].

2.2.3 Biodegradable natural polymers

a) Collagen

Collagen is the major component in connective tissues. Although it favours cell adhesion, the relatively fast *in vivo* degradation and loss of mechanical strength of this component, limit some application in tissue engineering [4].

However, due to the natural structure of the ACL, collagen-based fibre scaffolds are widely used for the replacement of this ligament. The mechanical strength and the control of the degradation rate of the scaffolds could be improved by cross-linking. Cross-links mechanically stabilize and improve the tensile strength of the collagen fibrils, enabling these tissues to resist deformation due stretching forces. [4, 32].

In 2001, the electro spinning of collagen was first reported. Since then, Sell et al. [14] have worked to demonstrate that the mentioned process has the potential to produce collagen fibres that closely mimic, and at some point may even fully reproduce, the structural and biological properties of the natural collagen ECM.

Blending collagen with other natural and/or synthetic polymers has enabled tissue engineers to fine tune the desired properties of the electro spun scaffolds.

b) Silk

Another natural polymer that has been proposed for tissue engineering of ACL is silk. This versatile biomaterial has very high tensile strength and resistance to failure in compression, as well as good biocompatibility, slow degradation and high crystallinity, which make them a good solution for ligament replacement. Moreover, according to some authors, silk fibres only lose the majority of their tensile strength after 1 year *in vivo* [4, 14, 32].

An ideal scaffold for ligament/tendon tissue engineering must be biodegradable, porous, have good mechanical properties (similar to those of natural ligaments) and promote the formation of biological tissue. Silk-based woven and knitted scaffolds have been studied and seem to have good chances to meet all of these requirements. PLGA-silk scaffold, for example, have shown potential to be further developed for use in ligament/tendon repair [14].

2.3 Viscoelastic models

Polymers and its composites, like the natural ligament tissue, show a viscoelastic behaviour, exhibiting elastic action upon loading (if loading is rapid enough), followed by a slow and continuous increase of strain at a decreasing rate. As its name implies, viscoelasticity combines elasticity and viscosity (viscous flow). Since time is a very important factor in their behaviour, they are also called time-dependent materials. The time-dependent behaviour of viscoelastic materials must be expressed by a constitutive equation which includes time as a variable in addition to the stress and strain variables. The time-dependent behaviour of viscoelastic materials can be studied by performing creep and stress relaxation tests [36].

Even under the simplest loading program, as shown in Figure 4, the shape of the strain-time curve, in this case a creep curve may be rather complicated. Since time cannot be kept constant, reversed or eliminated during an experiment, the experimental study of mechanical behaviour of such materials is much more difficult than the study of time-independent ones [36].

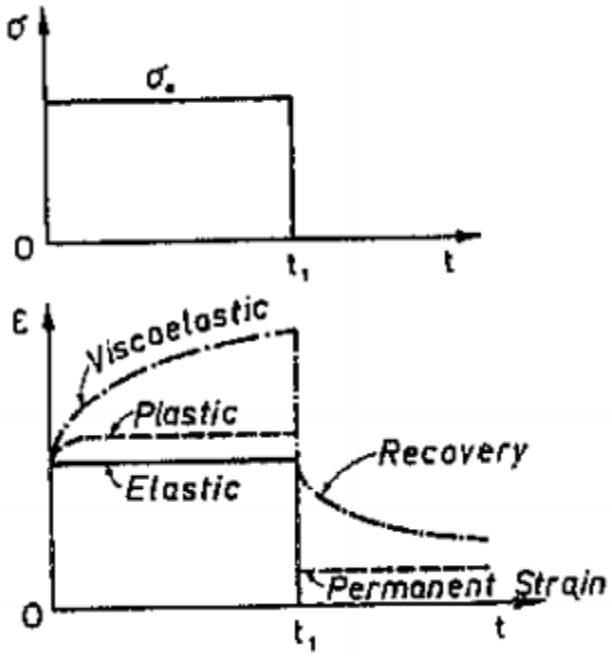

Figure 4 Various strain response to constant load [36]

Simple mechanical devices, such as linear springs and viscous dashpots, are widely used to create simple, practical viscoelastic models. These models are particularly successful to describe material behaviour under small stress levels where most of the materials exhibit linear or nearly linear behaviour. In recent years, there has been considerable activity to develop spring and dashpot models to describe soft biological tissue behaviour [21].

In this study, the mechanical model chosen to describe creep and stress relaxation data of PLA-PCL specimens was the four element model. The curve fitting procedure is presented in a later chapter.

2.3.1 Maxwell model

The Maxwell model is a two-element model consisting of a linear spring element and a linear viscous dashpot element connected in series as shown in Figure 5. The stress-strain relations of spring and dashpot are [36]

$$\sigma = R\varepsilon_s \tag{1}$$

$$\sigma = \eta \dot{\varepsilon}_d \tag{2}$$

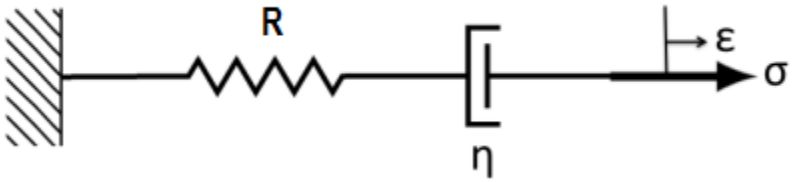

Figure 5 Maxwell model [21]

Since both are connected in series, the total strain is given by

$$\varepsilon = \varepsilon_s + \varepsilon_d \tag{3}$$

or the strain rate is

$$\dot{\varepsilon} = \dot{\varepsilon}_s + \dot{\varepsilon}_d \tag{4}$$

The following stress-strain rate relation for the Maxwell model is obtained by manipulating the equation (4), resulting in

$$\dot{\varepsilon} = \frac{\dot{\sigma}}{R} + \frac{\sigma}{\eta} \tag{5}$$

The strain-time relations under various stress conditions and stress-time relations under given strain input can be obtained by solving the differential equation (5). Applying a constant stress $\sigma = \sigma_0$ at $t = 0$, (5) becomes a first order differential equation of ε. The strain-time relation can be obtained after applying integration together with the initial condition $\sigma = \sigma_0$ at $t = 0$

$$\varepsilon(t) = \frac{\sigma_0}{R} + \frac{\sigma_0}{\eta} t. \tag{6}$$

If the Maxwell model is subjected to a constant strain ε_0 at the time $t = 0$, for which the initial value of the stress is σ_0, the stress response can be obtained by integrating (5) for these initial conditions with the following result

$$\sigma(t) = \sigma_0 e^{-Rt/\eta} = E\varepsilon_0 e^{-Rt/\eta} \tag{7}$$

2.3.2 Kelvin-Voigt model

The Kelvin-Voigt model is shown in Figure 6 where a spring element and a dashpot element are connected in parallel. The spring and dashpot have the following stress-strain relations [36]

$$\sigma_1 = \eta \dot{\varepsilon} \tag{8}$$

$$\sigma_2 = R\varepsilon \tag{9}$$

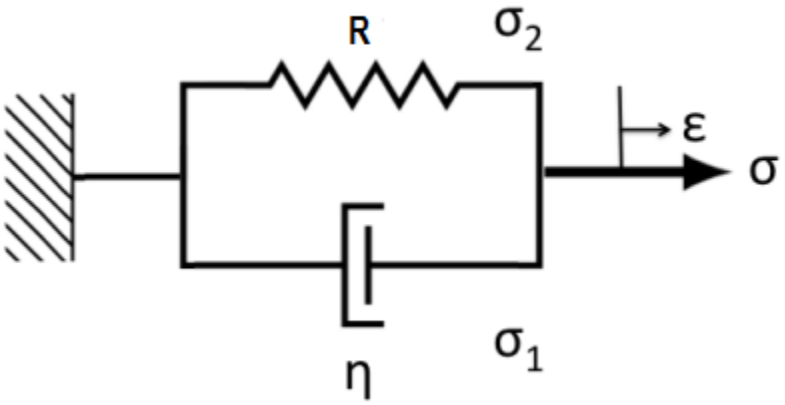

Figure 6 Kelvin-Voigt model [21]

Since both elements are connected in parallel, the total stress is

$$\sigma = \sigma_1 + \sigma_2 \tag{10}$$

and eliminating σ_1 and σ_2 the relation between σ and ε is given by

$$\dot{\varepsilon} + \frac{R}{\eta}\sigma = \frac{\sigma}{\eta} \tag{11}$$

For creep under constant stress σ_0 applied at $t = 0$, the solution of (11) is

$$\varepsilon(t) = \frac{\sigma_0}{R}(1 - e^{-Rt/\eta}). \tag{12}$$

The Kelvin-Voigt model does not show a time-dependent relaxation.

Neither the Maxwell nor the Kelvin-Voigt models accurately represents the behaviour of most viscoelastic materials. However, in order to understand the derivation of the next model presented, the four element model, these two models were first introduced since they represent the most basic cases of spring and dashpot models.

2.3.3 Burgers or four element model

The Burgers model is one of the most used models to give the relationship between the morphology of the composites and their creep behaviour. A representation of this model is shown in Figure 7, where a Maxwell and a Kelvin-Voigt model are connected in series. According to this method, the total strain as a function of time corresponds to the following equation [37, 38]:

$$\varepsilon = \varepsilon_1 + \varepsilon_2 + \varepsilon_3 \tag{13}$$

where

$$\varepsilon_1 = \frac{\sigma}{R_1} \tag{14}$$

$$\dot{\varepsilon}_2 = \frac{\sigma}{\eta_1} \tag{15}$$

$$\dot{\varepsilon}_3 + \frac{R_2}{\eta_2}\varepsilon_3 = \frac{\sigma}{\eta_2} \tag{16}$$

For the most general case of a linear viscoelastic solid, the total strain is the sum of three essentially separate parts: ε_1, the immediate elastic strain or instantaneous elasticity which appears instantly after loading and is gone after the load is removed; ε_2, the Newtonian flow, which is identical with the deformation of a viscous liquid obeying Newton's law of viscosity, and represents the irreversible creep strain in the element once it is subjected to a constant stress; ε_3, the delayed elasticity that increases under the applied stress, and is recovered once the stress is removed and the element is kept unloaded for an indefinite period of time. Equations (13) to (16) contain five unknowns $\varepsilon, \sigma, \varepsilon_1, \varepsilon_2, \varepsilon_3$. In principle, $\varepsilon_1, \varepsilon_2$ and ε_3 can be eliminated from these four equations yield a constitutive equation between σ and ε for the Burgers model with the following result [37-40]

$$\sigma + \left(\frac{\eta_1}{R_1} + \frac{\eta_1}{R_2} + \frac{\eta_2}{R_1}\right)\dot{\sigma} + \frac{\eta_1\eta_2}{R_1R_2}\ddot{\sigma} = \eta_1\dot{\varepsilon} + \frac{\eta_1\eta_2}{R_2}\ddot{\varepsilon} \tag{17}$$

The same result is shown in the following equation

$$\sigma + p_1\dot{\sigma} + p_2\ddot{\sigma} = q_1\dot{\varepsilon} + q_2\ddot{\varepsilon} \tag{18}$$

with

$$p_1 = \left(\frac{\eta_1}{R_1} + \frac{\eta_1}{R_2} + \frac{\eta_2}{R_1}\right) \tag{19}$$

$$p_2 = \frac{\eta_1\eta_2}{R_1R_2} \tag{20}$$

$$q_1 = \eta_1 \tag{21}$$

$$q_2 = \frac{\eta_1 \eta_2}{R_2} \tag{22}$$

The creep behaviour of this model under constant stress σ_0 can be obtained from equation (17) by solving this second order differential equation with two initial conditions

$$1.\ \varepsilon = \varepsilon_1 = \frac{\sigma_0}{R_1}, \quad \varepsilon_2 = \varepsilon_3 = 0, \quad t = 0 \tag{23}$$

$$2.\ \dot{\varepsilon} = \frac{\sigma_0}{\eta_1} + \frac{\sigma_0}{\eta_2} \tag{24}$$

Thus, the creep behaviour may be found to be as follows

$$\varepsilon = \sigma_0 \left[\frac{1}{R_1} + \frac{t}{\eta_1} + \frac{1}{R_2}(1 - e^{-R_2 t/\eta_2}) \right] \tag{25}$$

Here, t denotes time after loading, R_1 and η_1 are the modulus and viscosity of the Maxwell spring and dashpot, respectively; $\tau = \eta_2 / R_2$ is the retardation time taken to produce 63,2% or $(1 - e^{-1})$ of the total deformation in the Kelvin unit; R_2 and η_2 are the modulus and viscosity of the Kelvin spring and dashpot, respectively [37, 38].

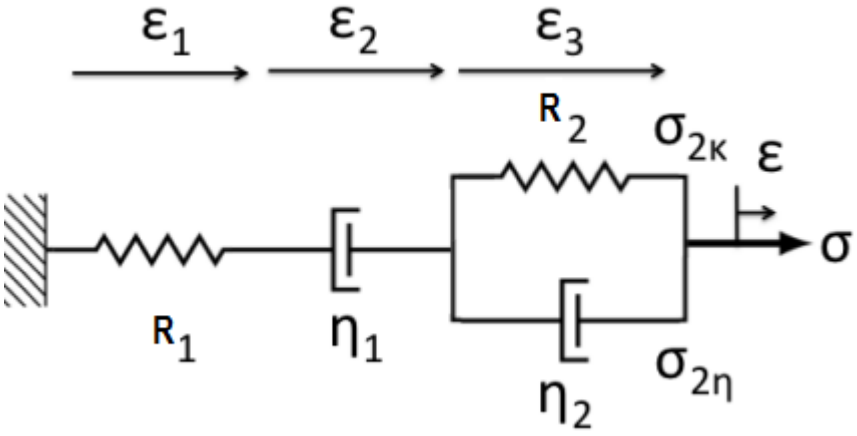

Figure 7 Four element model or Burgers model [21]

3 Mechanical tests

As it was already mentioned, an artificial tissue as a ligament must have such requirements, like being biocompatible, nontoxic, and display a similar mechanical behaviour (shape of stress-strain and stress-relaxation response).

In order to study PLA-PCL mechanical behaviour, specimens were subjected to static and dynamic mechanical analysis, by means of tensile, creep and stress relaxation tests. All tests were performed at room temperature, in an Instron ElectroPuls E1000 machine (from LABIOMEP, Porto Biomechanics Laboratory, University of Porto). According to protocol, the same experimental test was repeated for three different PLA-PCL specimens (Figure 8), both in static and dynamic tests.

Table 7 Specimens dimensions and saturation time

Total length	80 mm
Gauge length	50 mm
Diameter	0.505 mm
Saturation time (for saturated specimen)	≥ 120 min

For mechanical tests with saturated specimens, the medium used to soak the PLA-PCL fibres was physiologic saline solution. During this tests, a dropper was used to moisten the fibres and efforts were made to ensure that they remained saturated throughout the mechanical tests.

Figure 8 PLA-PCL specimens

In order to keep the number of graphical representations to a minimum in the following sections, the information necessary for the proper analysis of the results obtained was handpicked. Additional graphs can be found in Annex A

3.1 Tensile tests results

The tensile test results are graphically represented in Figure 9 and Figure 10. Table 8 summarizes the main mechanical properties such as nominal strain and stress at failure and Young modulus. These tests were performed with a 2 kN load cell, in displacement control, up to rupture, with a displacement rate of 5 mm/min.

Table 8 Mechanical properties of PLA-PCL specimens

	Young Modulus (GPa)	St. Dev.	Max. Strain (%)	St. Dev.	Max. Stress (MPa)	St. Dev.
DRY						
Specimen 1	1.58		76.57		253.98	
Specimen 2	1.68		76.91		237.75	
Specimen 3	1.74		88.09		275.53	
Average	***1.67***	*0.07*	***80.52***	*5.35*	***255.75***	*15.47*
SATURATED						
Specimen_SAT 1	1.50		79.67		242.59	
Specimen_SAT 2	1.47		77.40		232.51	
Specimen_SAT 3	1.36		77.58		232.22	
Average	***1.44***	*0.06*	***78.21***	*1.03*	***235.77***	4.82

The values presented in Table 8 show that saturating the fibres results in a decrease of the mechanical properties. The water acts as an internal lubricant resulting in degradation of mechanical properties.

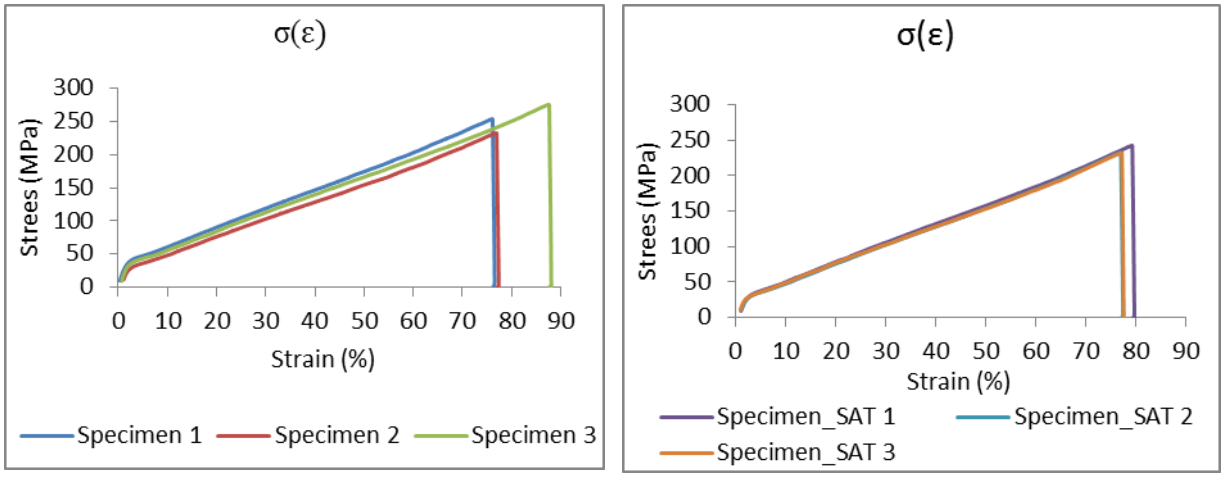

a) **b)**

Figure 9 Results of the tensile tests for: **a)** dry specimens **b)** saturated specimens

The graphics of Figure 9 present the engineering stress (σ) as a function of the engineering strain (ε). Knowing that true stress (σ_T) and engineering stress (ε_T) are related by

$$\sigma_T = \sigma(1+\varepsilon) \tag{26}$$

and that the true strain and the engineering strain are related by

$$\varepsilon_T = \ln(1+\varepsilon) \tag{27}$$

The same results are presented in Figure 10 as $\sigma_T = f(\varepsilon_T)$. This graph evidences the nonlinear behaviour of the composite material.

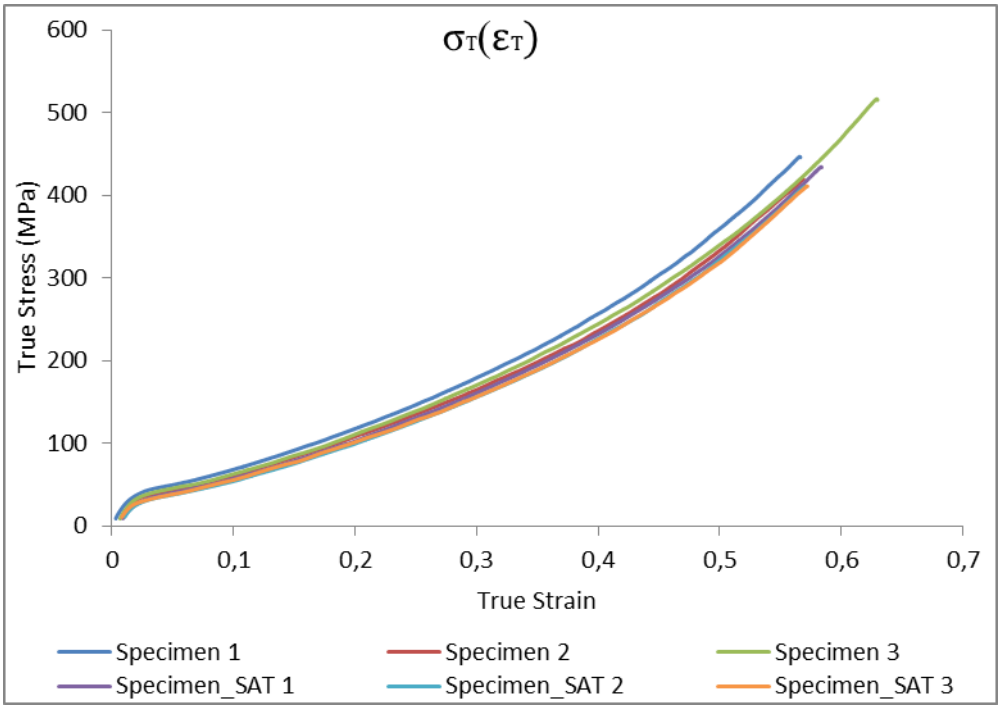

Figure 10 Stress-strain curves of PLA-PCL specimens

3.2 Dynamic tests

The knowledge of the mechanical properties was important to define the different stages for the creep and stress relaxation tests. The values chosen for maximum strain and stress were the lowest obtained in the tensile tests, at expense of averaging values. Thus, it is intended to assure that the specimens don't break too soon, even when there might have been slight variations in length for the specimen tested. According to the data presented in Table 8, the values considered for the maximum strain and stress of the dry specimens test were:

$$\varepsilon_{máx.} = 76.57\% \tag{28}$$

$$\sigma_{máx.} = 237.75MPa \tag{29}$$

and for the tests with saturated specimens, the maximum strain and stress were:

$$\varepsilon_{máx.} = 77.40\% \tag{30}$$

$$\sigma_{máx.} = 232.22MPa \tag{31}$$

The different levels of creep and stress relaxation tests performed are shown schematically in the flowchart of Figure 11.

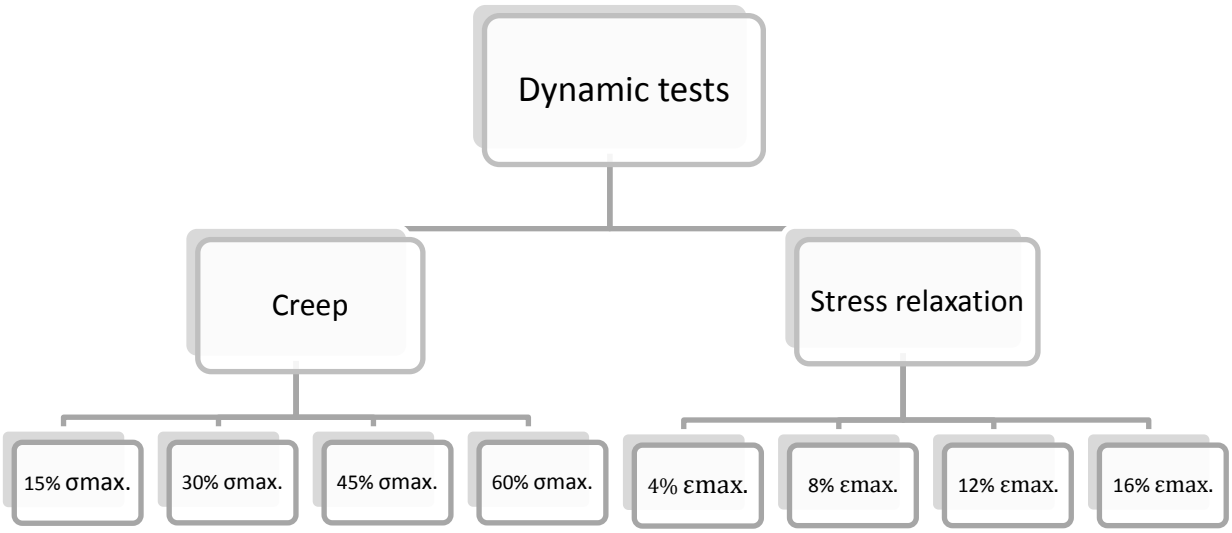

Figure 11 Flowchart: Dynamic tests

Table 9 shows the input stress or input strain value for each level of test (creep or stress relaxation, respectively) based on the maximum values previously calculated.

Table 9 Stress and strain input values

Test	Level	Input		
		% $\sigma_{max.}$/ $\varepsilon_{max.}$	*Values for tests with dry specimens*	*Values for tests with saturated specimens*
Creep				
T1	1	15% $\sigma_{max.}$	35.66 MPa	34.83 MPa
T2	2	30% $\sigma_{max.}$	71.32 MPa	69.67 MPa
T3	3	45% $\sigma_{max.}$	106.99 MPa	104.50 MPa
T4	4	60% $\sigma_{max.}$	142.65 MPa	139.33 MPa
Stress Relaxation				
D1	1	4% $\varepsilon_{max.}$	3.06 %	3.10 %
D2	2	8% $\varepsilon_{max.}$	6.13 %	6.19 %
D3	3	12% $\varepsilon_{max.}$	9.19 %	9.29 %
D4	4	16% $\varepsilon_{max.}$	12.25 %	12.38 %

3.2.1 Creep tests results

a) Dry specimens

The testing protocol for the creep tests is illustrated in Figure 12. According to the level of the experimental test (see Table 9), the specimens were loaded to 15, 30, 45 or 60% of maximum stress. The PLA-PCL fibres were ramped up to the input stress in 1.2 seconds, then kept at the this level for, approximately, 600 seconds and, after this holding phase, they were ramped down reaching the 0 stress after another 600 seconds.

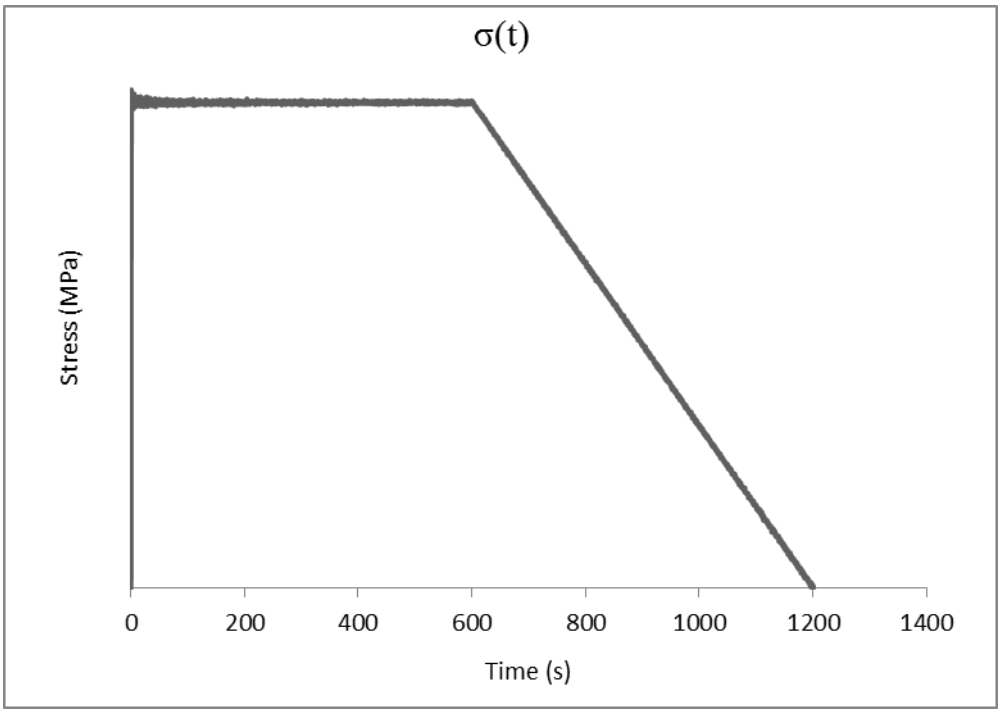

Figure 12 The input stress protocol for the PLA-PCL creep tests

Figure 13 illustrates the results obtained in all the these experimental tests (three PLA-PCL fibres per level) and is divided into four different graphs, each one corresponding to a different level of experimental test. In Figure 14, for each level of stress input, an average of the results obtained from the testing of three specimens is shown.

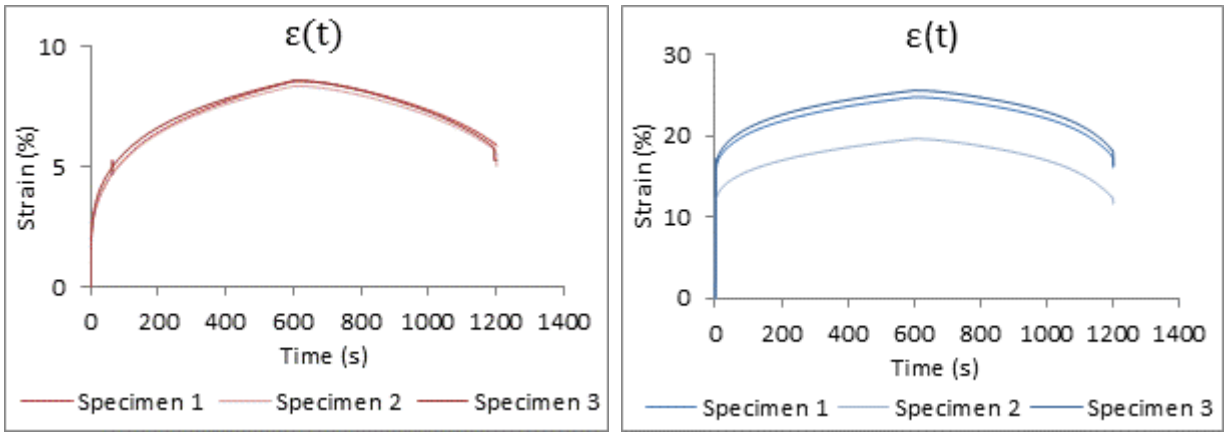

a) **b)**

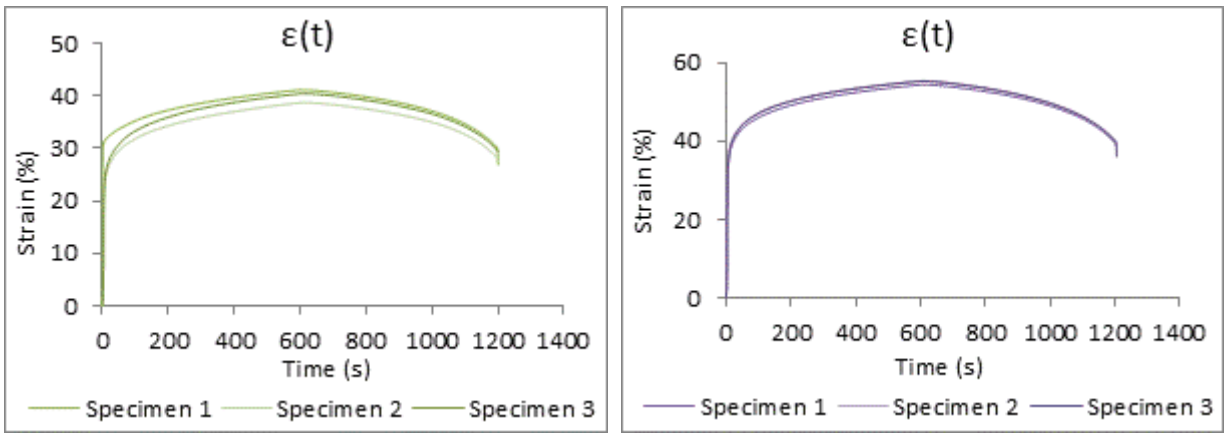

c) **d)**

Figure 13 Creep behaviour under: **a)** 15% $\sigma_{max.}$; **b)** 30% $\sigma_{max.}$; **c)** 45% $\sigma_{max.}$; **d)** 60% $\sigma_{max.}$ (dry specimens)

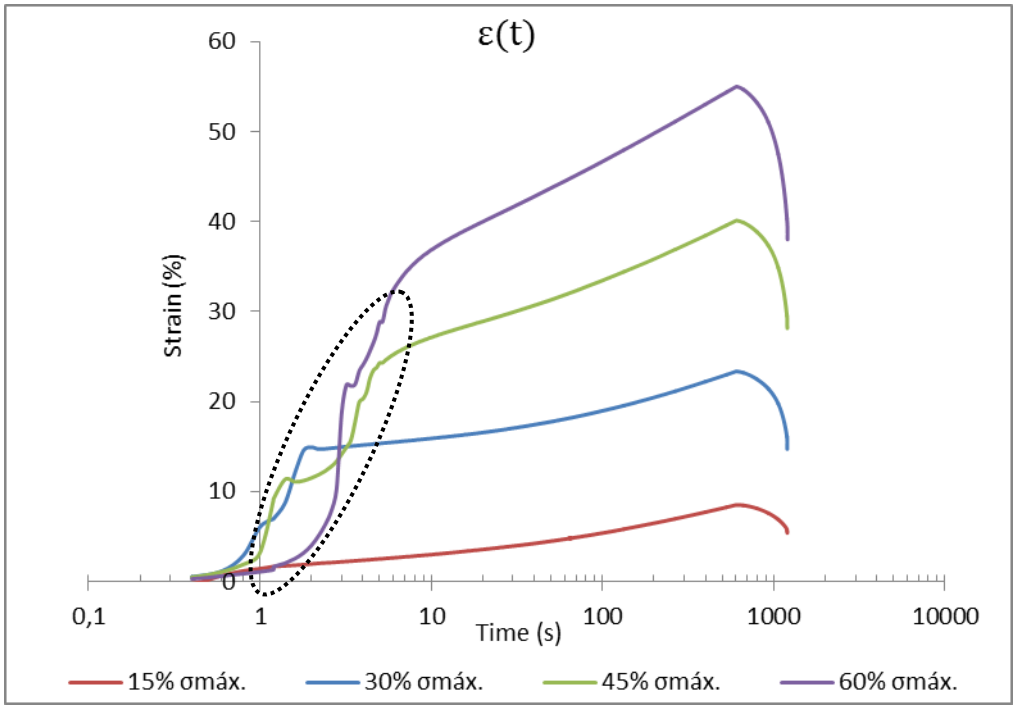

Figure 14 Creep at multiple levels of stress – 3 specimens' data average (dry specimens)

While the material is submitted to a constant load, independently of its value, the fibres suffer an increase in strain. When load decreases, around the 600 seconds mark, so does strain and, at the end of the test, the specimens are characterized by what is designated as permanent strain.

The erratic behaviour of the curves found in the early stage of the tests (as highlighted in Figure 14) may be associated with slip phenomena of the samples during the mechanical test, since the grips are not meant for fibres. This behaviour is amplified by the increasing speed of the test in this stage.

In Figure 15 is represented the most linear region of the different creep curves in a Log-Log scale from which we can conclude that the rate of creep decreases as the stress level is increased.

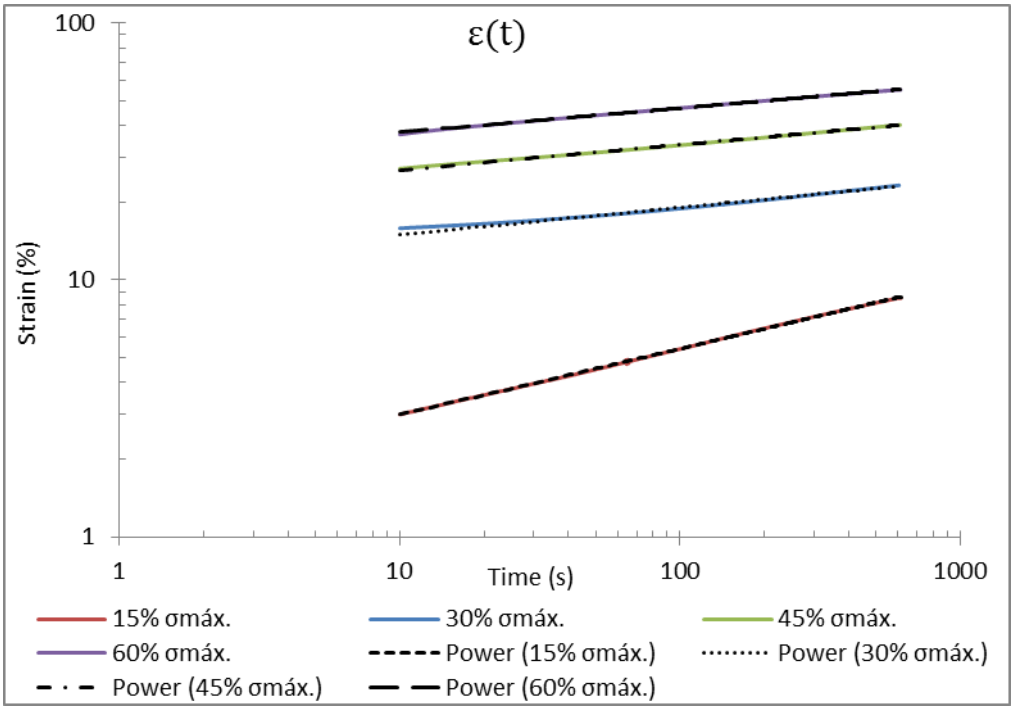

Figure 15 Creep at multiple levels of stress (Log–Log scale) – 3 specimens' data average (dry specimens)

The strain (in %) and rate of creep (n) for each of these four tests is represented by the following equations:

Power (15% $\sigma_{max.}$): σ=35.66 MPa; $\varepsilon=1.6546xt^{0.2568}$; $R^2=0.9996$

Power (30% $\sigma_{max.}$): σ=71.32 MPa; $\varepsilon=11.764xt^{0.1058}$; $R^2=0.9917$

Power (45% $\sigma_{max.}$): σ=106.99 MPa; $\varepsilon=21.373xt^{0.098}$; $R^2=0.9991$

Power (60% $\sigma_{max.}$): σ=142.65 MPa; $\varepsilon=30.373xt^{0.0931}$; $R^2=0.9995$

The following equations were used to calculate the permanent (ε_p) and the recoverable strain (ε_r).

$$\varepsilon_p = \varepsilon_{t\approx 1200s} \tag{32}$$

$$\varepsilon_{máx.} = \varepsilon_{t\approx 600s} \tag{33}$$

$$\varepsilon_r = \varepsilon_{máx.} - \varepsilon_p \tag{34}$$

Table 10 Permanent strain and recoverable strain (dry specimens)

Strain	Creep level			
	T1	*T2*	*T3*	*T4*
ε_p (%)	5.402	14.719	28.160	38.024
ε_{max} (%)	8.510	23.353	40.127	55.023
ε_r (%)	3.108	8.634	11.967	16.999

The values of Table 10, calculated based on the information present in Figure 14, show that both permanent and recoverable strain increase with input stress.

b) Saturated specimens

For creep testing of the saturated specimens, the protocol was similar to the previous one, but this time the fibres were ramped up to the input stress in 5.2 seconds. This slight change was introduced to try to mitigate the "overshoot" of the input stress before stabilizing at the desired value.

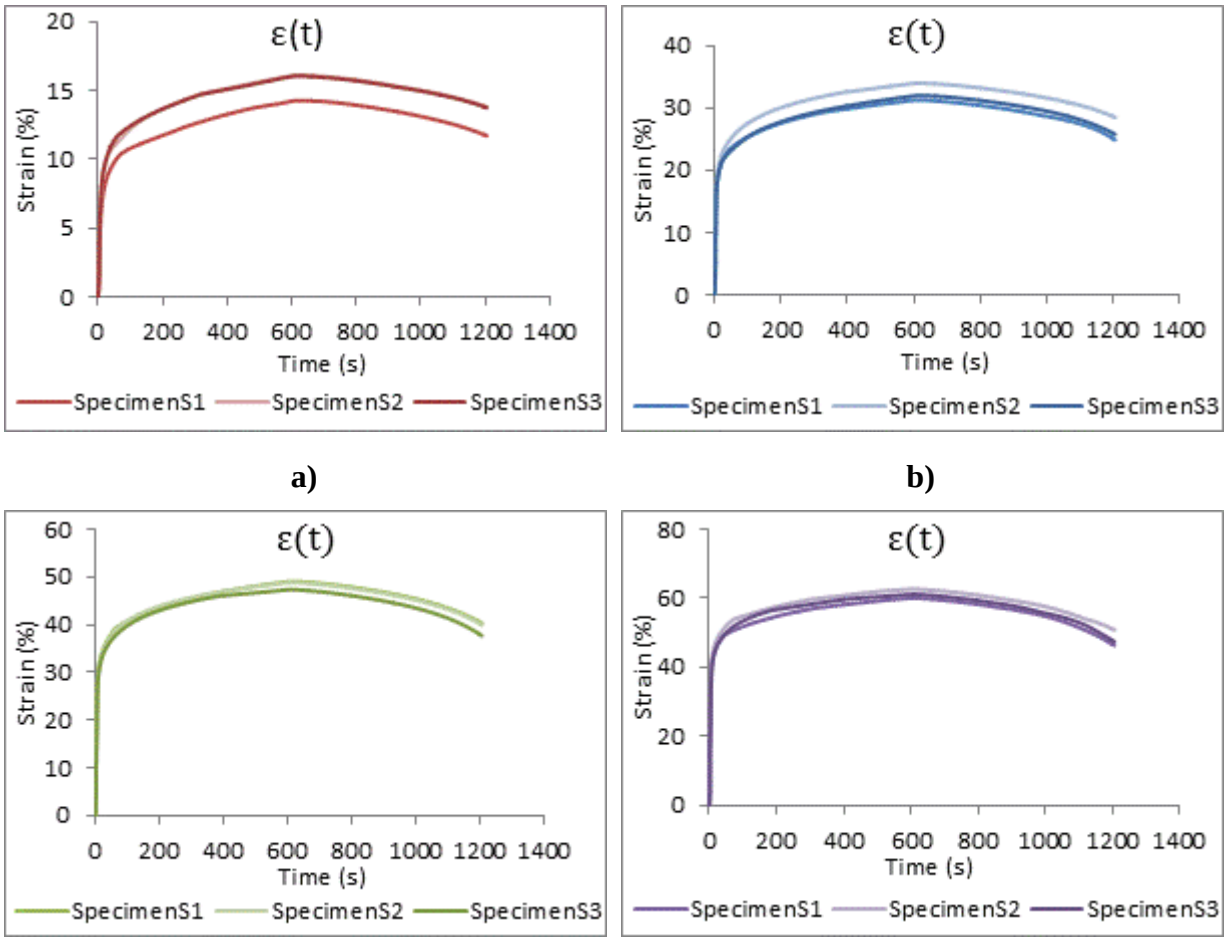

Figure 16 Creep behaviour under: **a)** 15% $\sigma_{max.}$; **b)** 30% $\sigma_{max.}$; **c)** 45% $\sigma_{max.}$; **d)** 60% $\sigma_{max.}$ (saturated specimens)

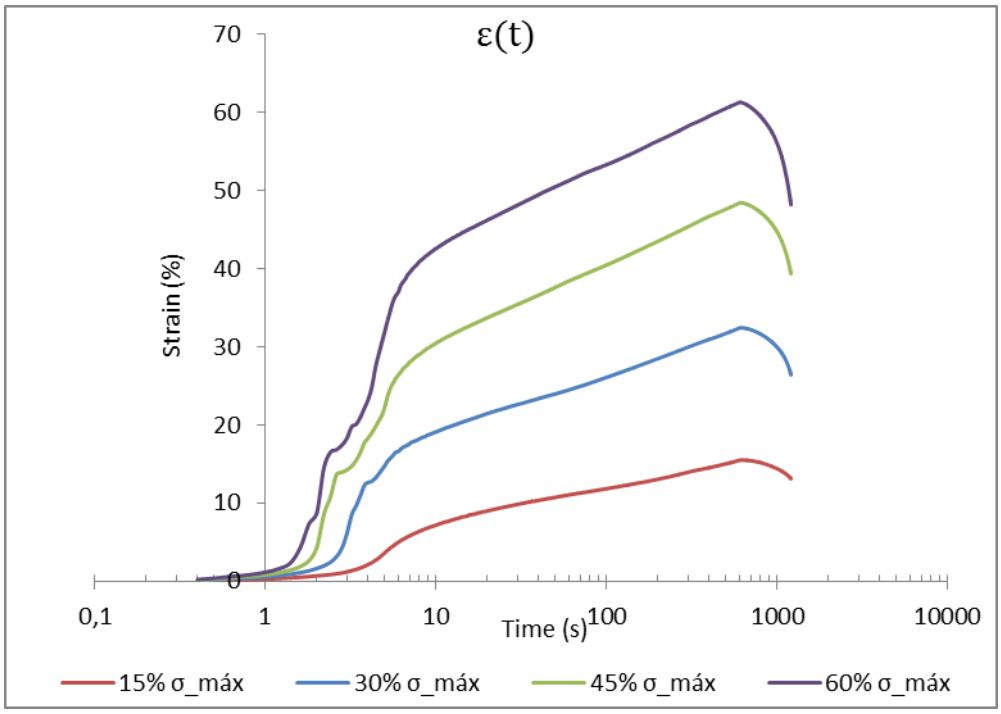

Figure 17 Creep at multiple levels of stress – 3 specimens' data average (saturated specimens)

When compared with creep testing data of dry specimens, data of saturated specimens shows a slight increase in the response. It is important to note that along with this increase it so happens that the maximum stress is slightly lower for the saturated specimens.

In Figure 18 is represented the most linear region of the different creep curves in a Log-Log scale.

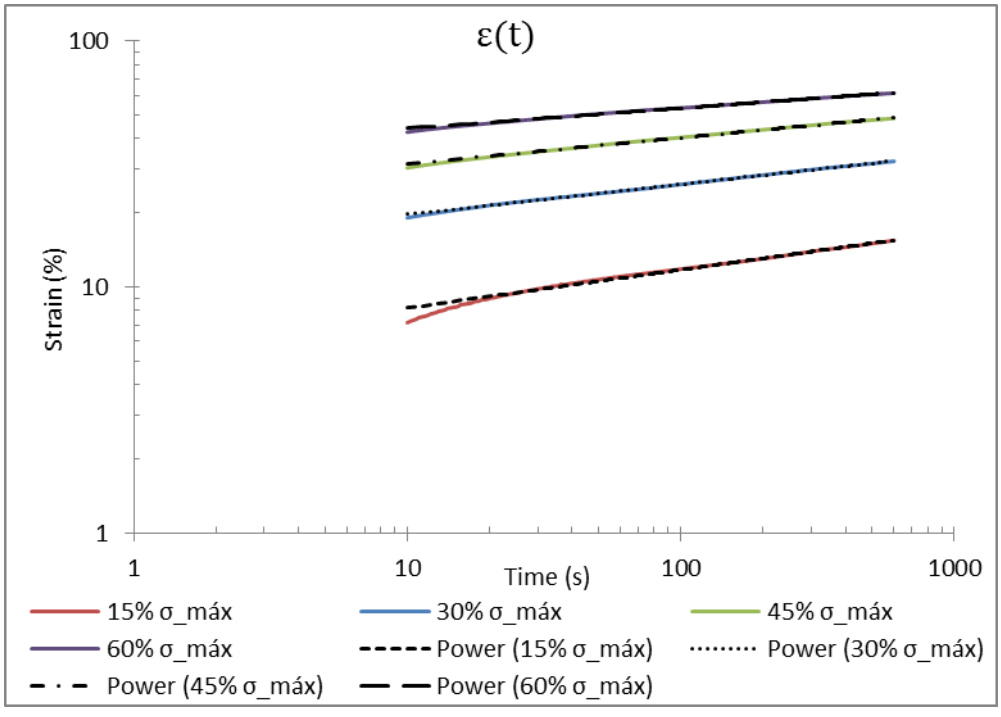

Figure 18 Creep at multiple levels of stress (Log–Log scale) – 3 specimens' data average (saturated specimens)

The rate of creep tends to decrease as the stress level is increased. The strain (in %) and rate of creep (n) for each of these four tests is represented by the following equations:

Power (15% $\sigma_{max.}$): σ=34.83 MPa; $\varepsilon=5.741xt^{0.1547}$; R^2=0.9937

Power (30% $\sigma_{max.}$): σ=69.67 MPa; $\varepsilon=14.837xt^{0.1224}$; R^2=0.9992

Power (45% $\sigma_{max.}$): σ=104.50 MPa; $\varepsilon=24.862xt^{0.1049}$; R^2=0.9977

Power (60% $\sigma_{max.}$): σ=139.33 MPa; $\varepsilon=36.539xt^{0.0813}$; R^2=0.9976

Table 11 Permanent strain and recoverable strain (saturated specimens)

Strain	Creep level			
	T1	*T2*	*T3*	*T4*
ε_p (%)	13.085	26.361	39.289	48.130
ε_{max} (%)	15.470	32.387	48.385	61.254
ε_r (%)	2.385	6.026	9.096	13.124

As previously verified for dry specimens, permanent and recoverable strain increase with input stress.

3.2.2 Stress relaxation tests results

a) Dry Specimens

The testing protocol for the stress relaxation tests is illustrated in Figure 19. According to the level of the experimental test (see Table 9), the specimens were stretched to 4, 8, 12 or 16% of maximum strain. The PLA-PCL fibres were ramped up to the input strain in 1.2 seconds, then kept at the this level for, approximately, 300 seconds and, after this holding phase, they were ramped down reaching the 0% strain after another 300 seconds.

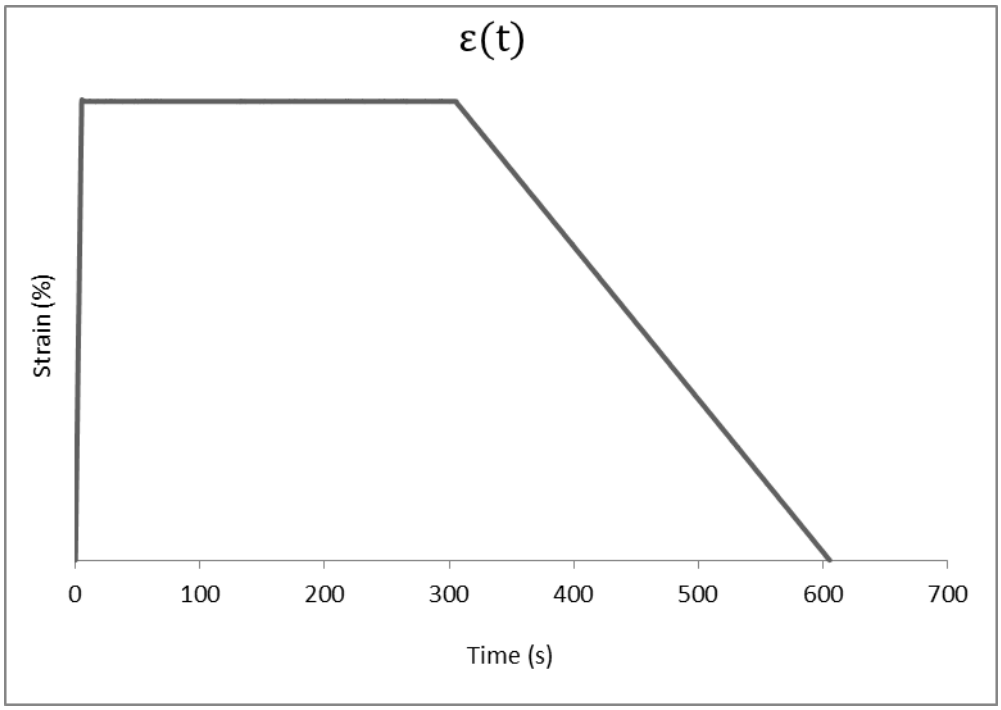

Figure 19 The input strain protocol for the PLA-PCL stress relaxation tests

As it was done for the creep tests, in Figure 20 are presented the results from the twelve tests performed and in Figure 21, for each level of strain input, an average of the results obtained from the testing of three specimens is shown.

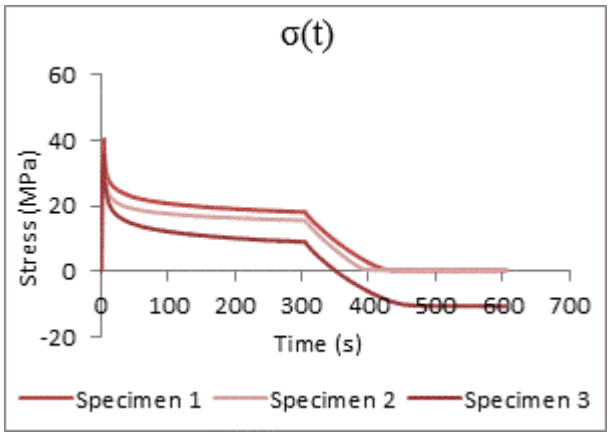

a)

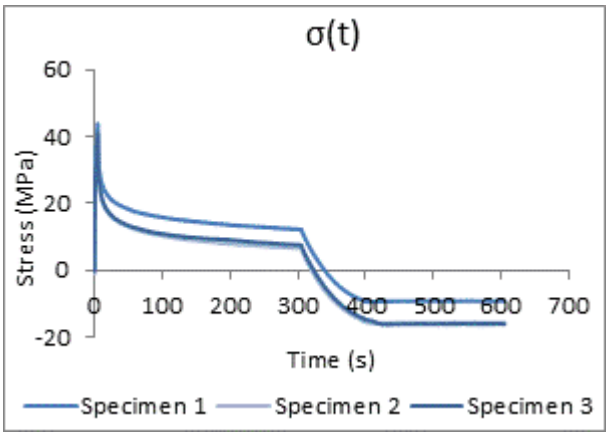

b)

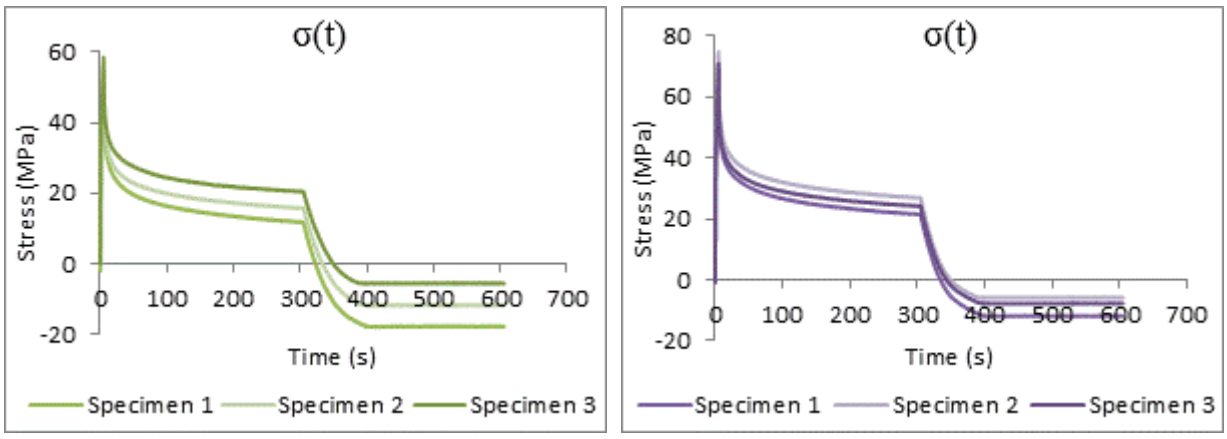

c) **d)**

Figure 20 Stress relaxation behaviour under: **a)** 4% $\varepsilon_{max.}$; **b)** 8% $\varepsilon_{max.}$; **c)** 12% $\varepsilon_{max.}$; **d)** 16% $\varepsilon_{max.}$ (dry specimens)

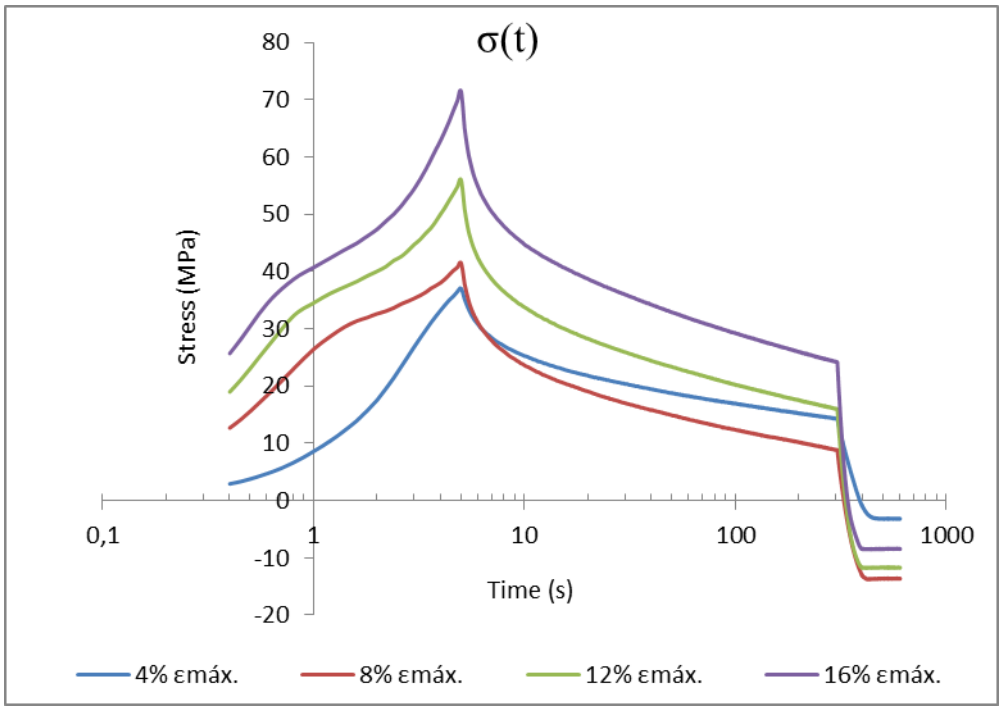

Figure 21 Stress relaxation at multiple levels of strain – 3 specimens' data average (dry specimens)

From the analysis of Figure 20, it follows that all the curves show two distinct phases of behaviour (the first one that goes from 0 to 300 seconds, and the second one that goes from 300 seconds forward) that are directly related to the behaviour of the strain input. In general, at least during the first phase of mechanical testing, stress is higher for those levels where the input strain is higher.

On the basis of the explanation for the negative values that appear in the second half of the graph may be the phenomenon of buckling observed in the tested fibres as a result of a decrease in strain (see Figure 23).

In Figure 22 is represented the most linear region of the different stress relaxation curves in a Log-Log scale from which we can conclude that the rate of relaxation tends to decrease as the strain level is increased.

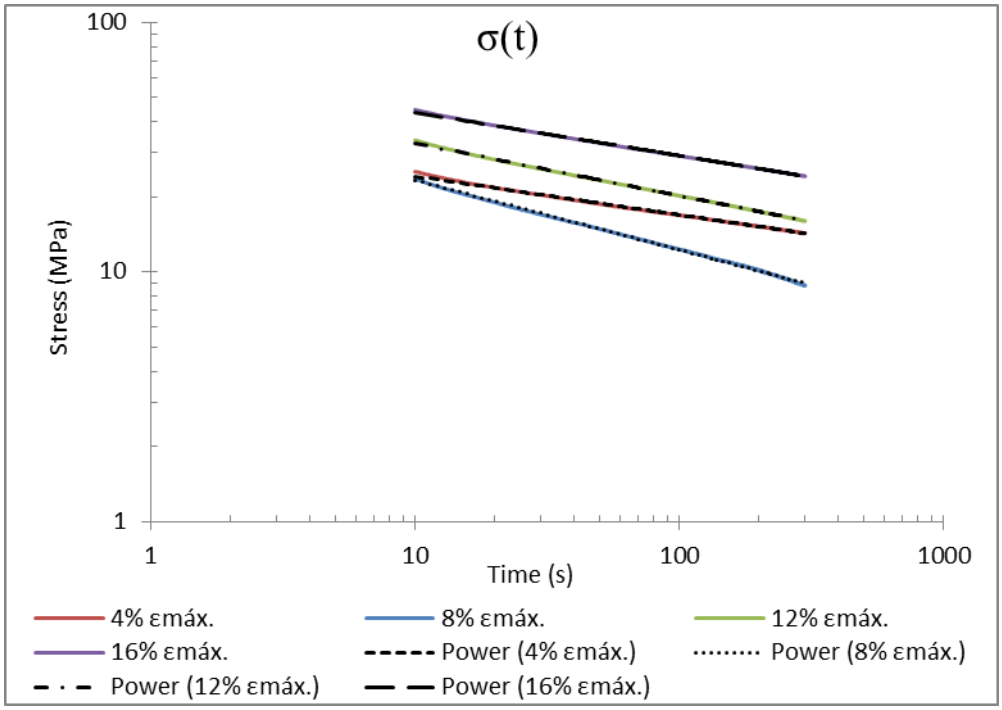

Figure 22 Stress relaxation at multiple levels of strain (Log–Log scale) – 3 specimens' data average (dry specimens)

The stress (in MPa) and rate of relaxation (n) for each of these four tests is represented by the following equations:

Power (4% $\varepsilon_{max.}$): ε =3.06%; $\sigma=34.563xt^{-0.155}$; $R^2=0.9984$

Power (8% $\varepsilon_{max.}$): ε=6.13%; $\sigma=44.51xt^{-0.28}$; $R^2=0.9984$

Power (12% $\varepsilon_{max.}$): ε=9.19%; $\sigma=53.119xt^{-0.21}$; $R^2=0.9996$

Power (16% $\varepsilon_{max.}$): ε=12.25%; $\sigma=64.853xt^{-0.173}$; $R^2=0.9996$

Figure 23 Buckling phenomenon observed in PLA-PCL fibres

b) Saturated Specimens

For stress relaxation testing of the saturated specimens, the protocol was analogous to the previous one, but similarly to what was done in creep tests, in these tests the specimens were ramped up to the input strain in 5.2 seconds. In Figure 24 are presented the results from the twelve tests performed and in Figure 25, for each level of strain input, an average of the results obtained from the testing of three specimens is shown.

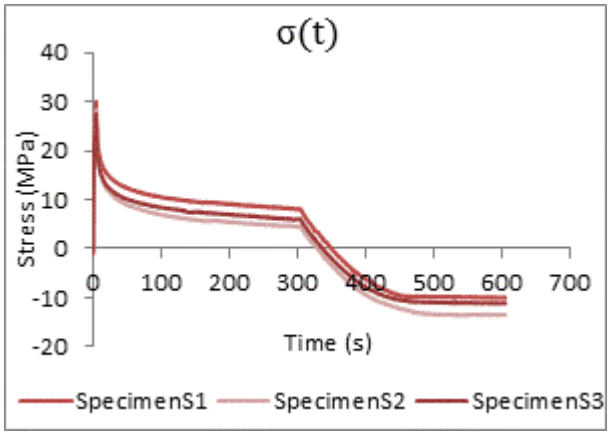

a)

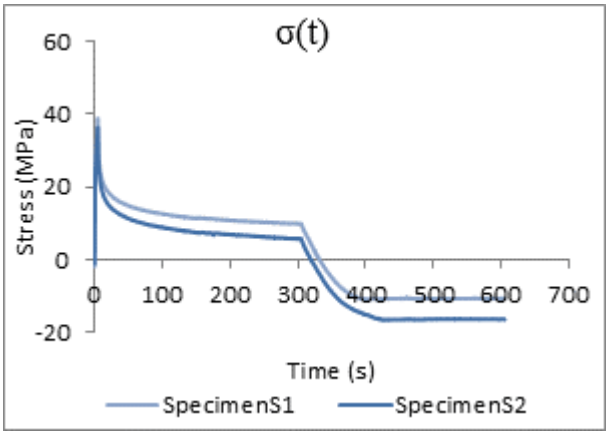

b)

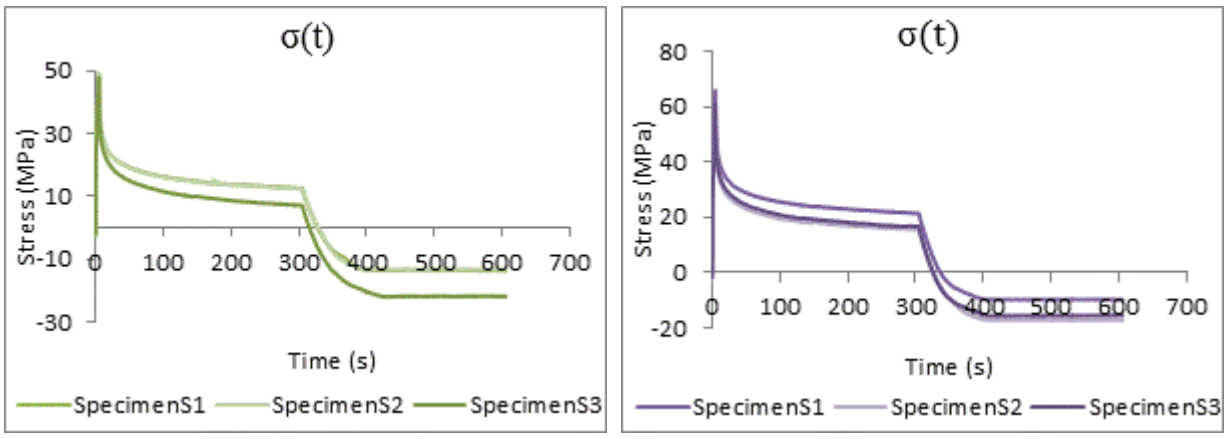

c) **d)**

Figure 24 Stress relaxation behaviour under: **a)** 4% $\varepsilon_{max.}$; **b)** 8% $\varepsilon_{max.}$; **c)** 12% $\varepsilon_{max.}$; **d)** 16% $\varepsilon_{max.}$ (saturated specimens)

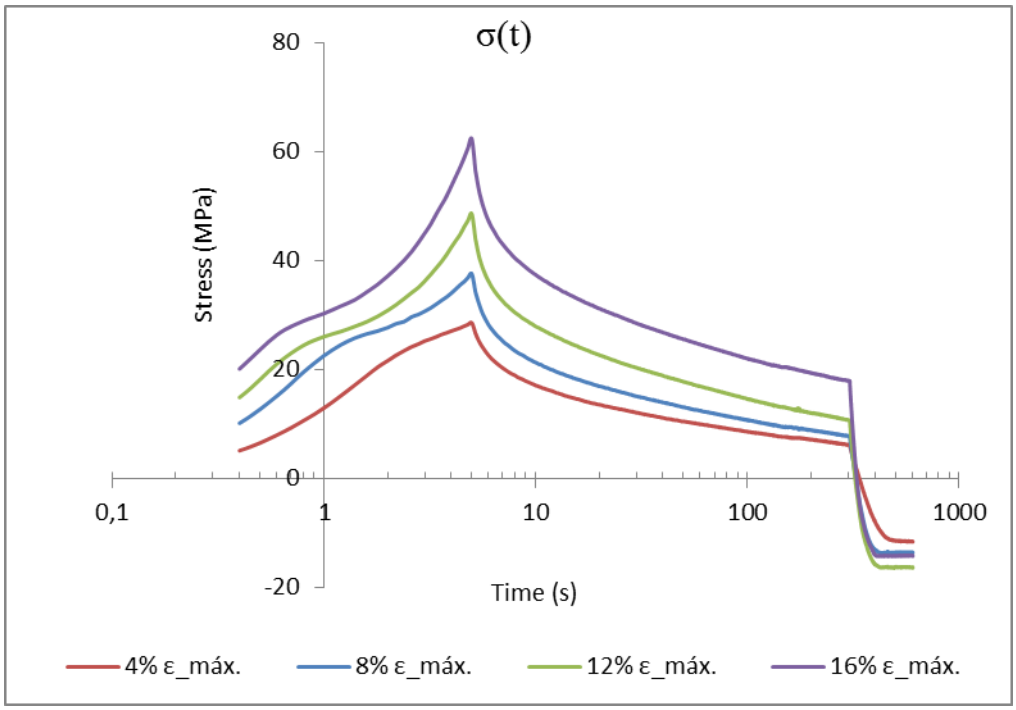

Figure 25 Stress relaxation at multiple levels of strain – 3 specimens' data average (saturated specimens)

When compared with stress relaxation testing data of dry specimens, data of saturated specimens shows a slight decrease in the response. It is important to note that along with this decrease it so happens that the maximum strain is slightly higher for the saturated specimens.

Table 12 shows that dry fibres have more pronounced stress relaxation than saturated fibres.

$$\Delta\sigma = \sigma_{máx.} - \sigma_{t\approx 300s} \tag{35}$$

Table 12 Stress drop according to specimen type and stress relaxation level

	Stress relaxation level			
	D1	*D2*	*D3*	*D4*
Δσ: *Dry specimens*	22.75	32.68	40.08	47.42
Δσ: *Saturated specimens*	22.39	29.75	37.82	44.45

In Figure 26 is represented the most linear region of the different stress relaxation curves in a Log-Log scale.

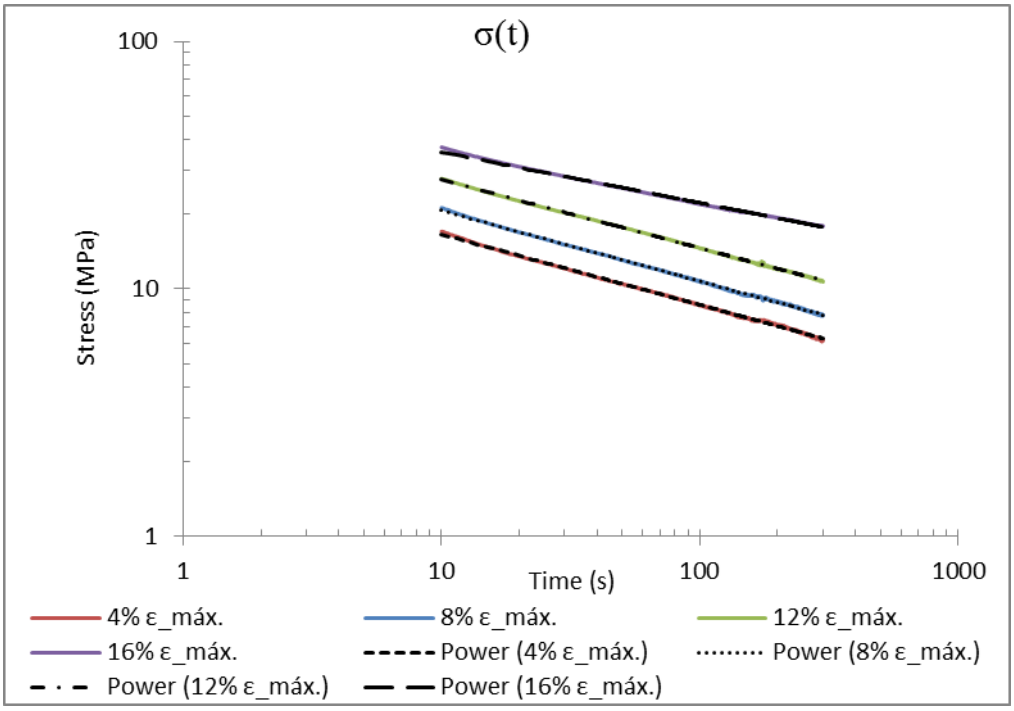

Figure 26 Stress relaxation at multiple levels of stress (Log–Log scale) – 3 specimens' data average (saturated specimens)

Once again, the rate of relaxation tends to decrease as the strain level is increased. The stress (in MPa) and rate of relaxation (n) for each of these four tests is represented by the following equations:

Power (4% $\varepsilon_{max.}$): ε =3.10%; $\sigma=31.995xt^{-0.285}$; $R^2=0.9984$

Power (8% $\varepsilon_{max.}$): ε=6.19%; $\sigma=39.98xt^{-0.285}$; $R^2=0.9991$

Power (12% $\varepsilon_{max.}$): ε=9.29%; $\sigma=52.261xt^{-0.277}$; $R^2=0.9996$

Power (16% $\varepsilon_{max.}$): ε=12.38%; $\sigma=57.013xt^{-0.204}$; $R^2=0.9976$

3.3 Conclusion

To sum up, it must be mentioned that the experimental tests performed for the PLA-PCL saturated fibres registered responses of slightly different values compared to dry specimens.

From the results obtained in the creep tests, we can conclude the rate of creep decreases as the stress level is increased and that saturation facilitates the deformation of the material. The stress relaxation data reveal that the rate of relaxation tends to decrease as the strain level is increased and that PLA-PCL dry specimens show more marked stress relaxation than saturated specimens.

It should be noted that saturating the fibres intends to simulate the moist environment found in the human body, if they were used as a ligament device.

4 Modelling

In this chapter, it is studied how successful the Burgers model is, a viscoelastic model presented in section 2.3.3, at predicting the stress relaxation behaviour of the PLA-PCL fibres based on creep experiments.

Using the MATLAB software, the processing of data obtained from experimental tests was made by means of a very simple program (ANNEX C) and with the Curve Fitting Tool (Figure 27). The results obtained in creep tests were compared with the equation that describes the creep behaviour of the Burgers model. This equation can be obtained by solving the second order differential equation (17) according to the input stress protocol established for creep tests. The itemized deduction can be found in ANNEX B. The parameters R_1, R_2, η_1 e η_2 are calculated after adjusting the Burgers equation to the experimental data.

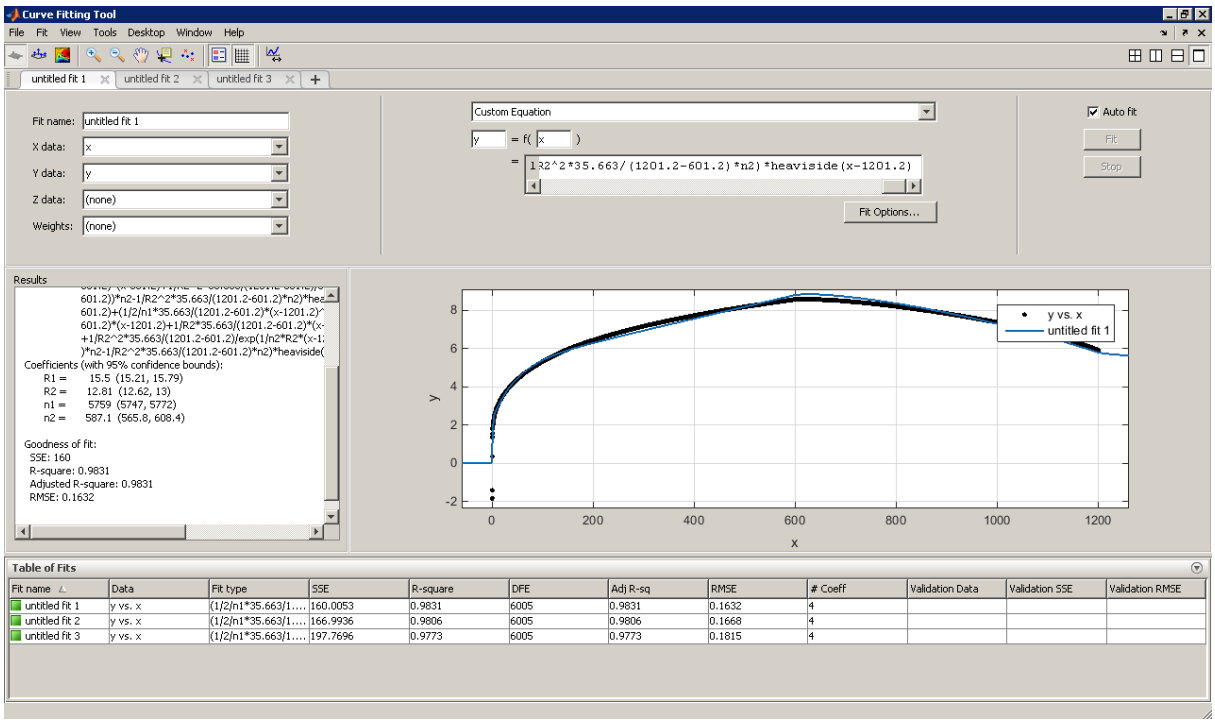

Figure 27 Curve Fitting Tool user interface

4.1 Dry specimens

Figure 28 shows the best fit of the Burgers equation to the results obtained in the first creep level.

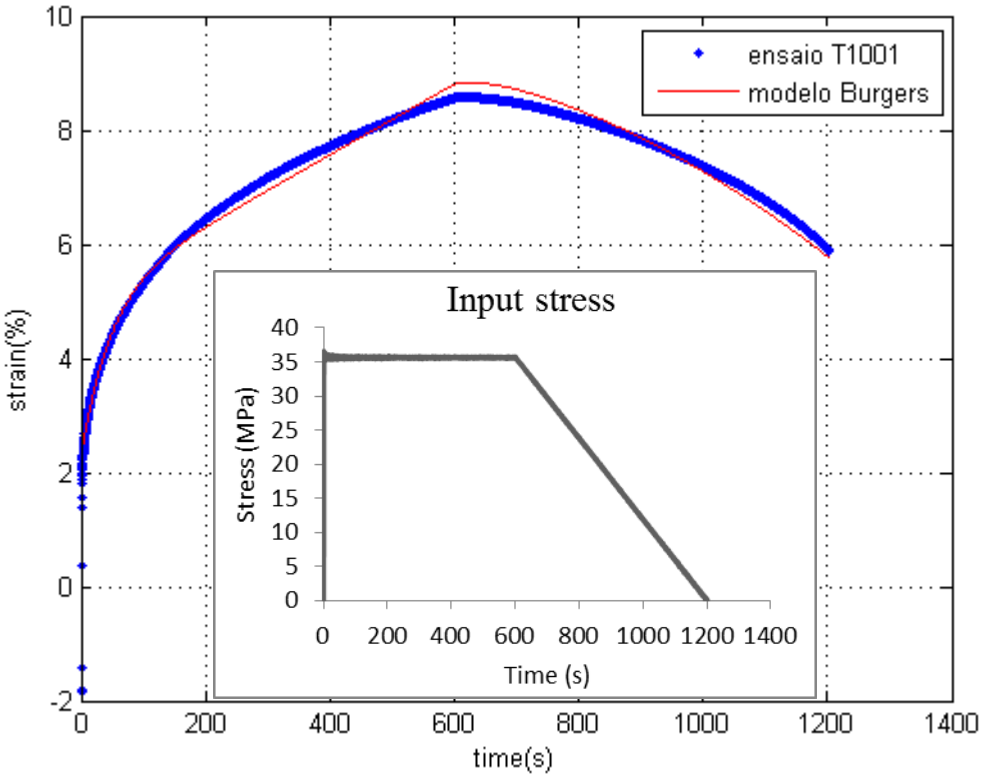

Figure 28 Best fit of the Burgers equation to the results obtained in the first creep level

For this test level, a good fit of the model to the experimental data is achieved. Since the Burgers model is a linear mechanical model, the PLA-PCL fibres appear to have a linear visco-elastic-plastic behaviour under small stress levels.

Table 13 Burgers model parameters with 95% confidence bounds for T1_00* tests

Test	R_1	St. Dev.	R_2	St. Dev.	η_1	St. Dev.	η_2	St. Dev.	R^2
T1_001	15.5	0.29	12.81	0.19	5759	12	587.1	21.3	0.9831
T1_002	15.28	0.29	13.06	0.21	6015	14	587.6	22.4	0.9806
T1_003	15.84	0.37	11.86	0.20	5916	14	449.6	18.2	0.9773
Average	***15.54***	*0.28*	***12.58***	*0.63*	***5896.67***	*129.09*	***541.43***	*79.53*	

On the other hand, at high stress levels the material seems to have a nonlinear behaviour that cannot be nicely described by a simple mechanical model like the four element model (see Figure 29).

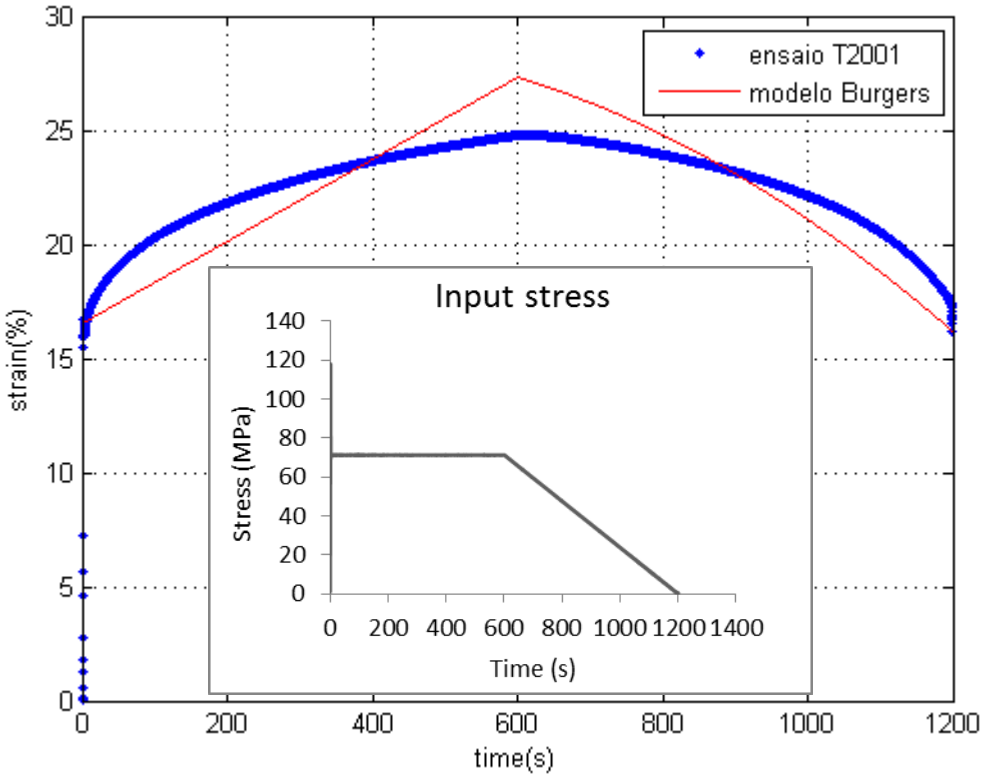

Figure 29 Best fit of the Burgers equation to the results obtained in the second creep level

The prediction of the stress relaxation behaviour is made with the Burgers model parameters, calculated for the first level of creep and presented in Table 13. Since a good model fit to the experimental data was achieved just for this first level of creep, we will assume that the values of these parameters are approximately constant. The ideal would be to get a good fit between model and experimental results for the multiple levels of creep in order to define each parameter as a function of the stress.

For a Burgers model, the total strain at time *t* will be the sum of the strain in the three elements (see Figure 7), where the spring and dashpot in the Maxwell model are considered as two elements [36]:

$$\varepsilon = \varepsilon_1 + \varepsilon_2 + \varepsilon_3 \tag{36}$$

$$\varepsilon_1 = \frac{\sigma}{R_1} \Rightarrow \dot{\varepsilon}_1 = \frac{\dot{\sigma}}{R_1} \tag{37}$$

$$\dot{\varepsilon}_2 = \frac{\dot{\sigma}}{\eta_1} \tag{38}$$

$$\dot{\varepsilon}_3 + \frac{R_2}{\eta_2}\varepsilon_3 = \frac{\sigma}{\eta_2} \tag{39}$$

Using the finite difference method,

$$\begin{cases} \dot{\varepsilon}_1 = \dfrac{\varepsilon(t_{j+1}) - \varepsilon(t)}{\Delta t} \\ \dot{\sigma}_1 = \dfrac{\sigma(t_{j+1}) - \sigma(t)}{\Delta t} \end{cases} \tag{40}$$

Replacing these two terms in equation (37), $\varepsilon_1(t_{j+1})$ is given by

$$\varepsilon_1(t_{j+1}) = \frac{1}{R_1}\sigma(t_{j+1}) \tag{41}$$

Using the same method, $\varepsilon_2(t_{j+1})$ and $\varepsilon_3(t_{j+1})$ are given by

$$\varepsilon_2(t_{j+1}) = \frac{\Delta t}{\eta_1}\sigma(t_{j+1}) + \varepsilon_2(t_j) \tag{42}$$

$$\varepsilon_3(t_{j+1}) = \frac{\dfrac{\Delta t}{\eta_2}\sigma(t_{j+1}) + \varepsilon_3(t_j)}{1 + \dfrac{R_2}{\eta_2}\Delta t} \tag{43}$$

Thus, the total strain at time t_{j+1} is

$$\varepsilon(t_{j+1}) = \varepsilon_1(t_{j+1}) + \varepsilon_2(t_{j+1}) + \varepsilon_3(t_{j+1}) \tag{44}$$

Imposing that $\varepsilon(t_{j+1})$ equals to the experimental strain, stress relaxation behaviour can be predicted by the following equation:

$$\sigma(t_{j+1}) = \frac{\varepsilon(t_{j+1}) - \varepsilon_2(t) - \varepsilon_3(t)\dfrac{\eta_2}{\eta_2 + R_2\Delta t}}{\dfrac{1}{R_1} + \dfrac{\Delta t}{\eta_1} + \dfrac{\Delta t}{\eta_2 + R_2\Delta t}} \tag{45}$$

and replacing R1, R2, η1 e η2 with the average values determined in Table 13,

$$\sigma(t_{j+1}) = \frac{\varepsilon(t_{j+1}) - \varepsilon_2(t) - \varepsilon_3(t)\dfrac{541.43}{541.43 + 12.58\Delta t}}{\dfrac{1}{15.54} + \dfrac{\Delta t}{5896.67} + \dfrac{\Delta t}{541.43 + 12.58\Delta t}} \tag{46}$$

Figure 30 shows the model's best prediction of stress relaxation behaviour in the first stress relaxation level.

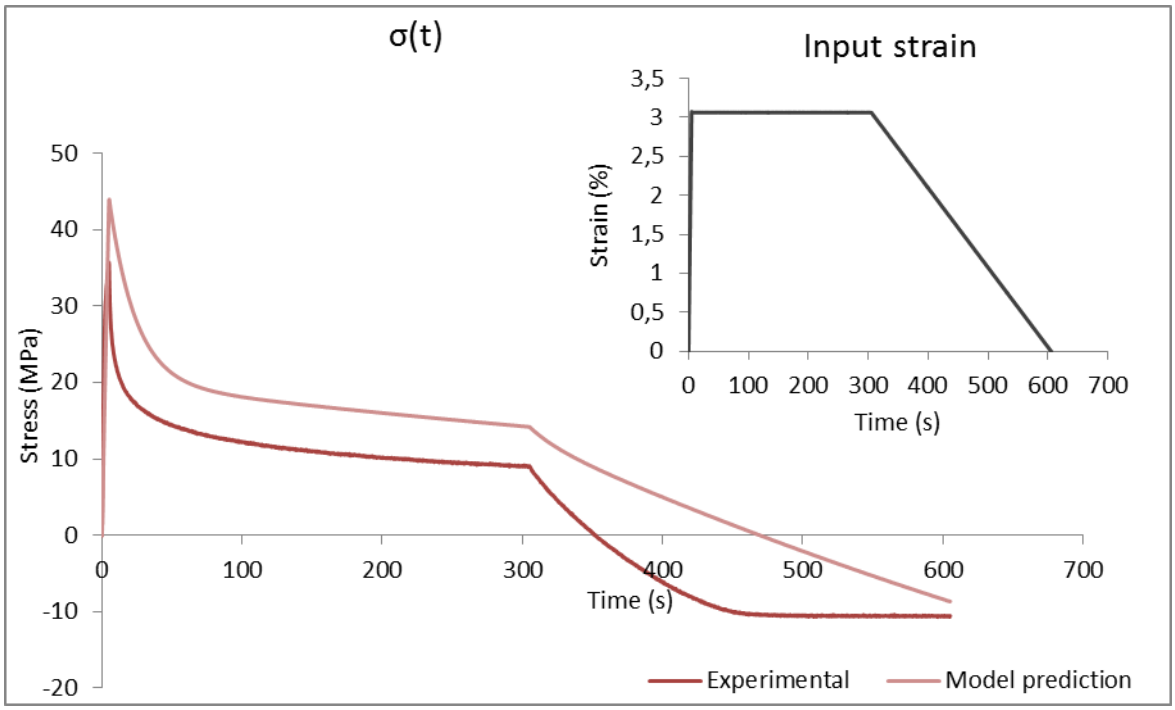

Figure 30 Burgers model best prediction of stress relaxation behaviour in the first stress relaxation level

For the first 300 seconds, the model prediction is quite reasonable. Even with some difference between predicted and experimental values, the shape of the two curves is very similar. As such, for this first stress relaxation level, it is presumable that the values obtained for the Burgers parameters from the first creep level are not far from the actual values.

In the period corresponding to the second part of the mechanical test, both behaviour and values of the prediction curve deviate from the experimental results.

In this chapter, we will not worry about predicting experimental negative results.

Figure 31 shows the Burgers model best prediction of stress relaxation behaviour in the second stress relaxation level.

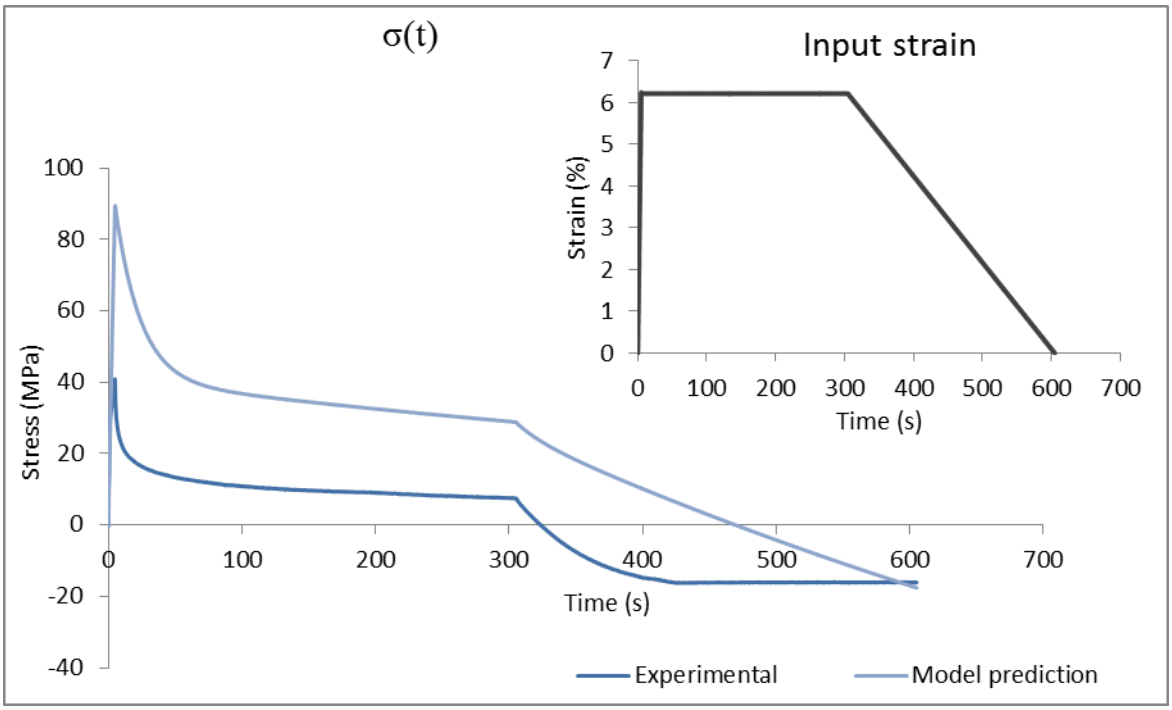

Figure 31 Burgers model best prediction of stress relaxation behaviour in the second stress relaxation level

Once again, in this second level of stress relaxation, the behaviour of the predicted curve and the experimental one is very similar. However, in this case, the discrepancy between experimental and calculated values is way more pronounced. This leads us to conclude that, for this level, the values that were initially assumed for the Burgers parameters are quite different from the real ones.

Additionally, 3 cycles of stress relaxation with different strain steps were performed (Figures 32 – 35). The behaviour of the model at predicting these experimental results was also analysed.

- **Cycle 1**
  - Step 1: 4% $\varepsilon_{max.}$
  - Step 2: 8% $\varepsilon_{max.}$
  - Step 3: 4% $\varepsilon_{max.}$

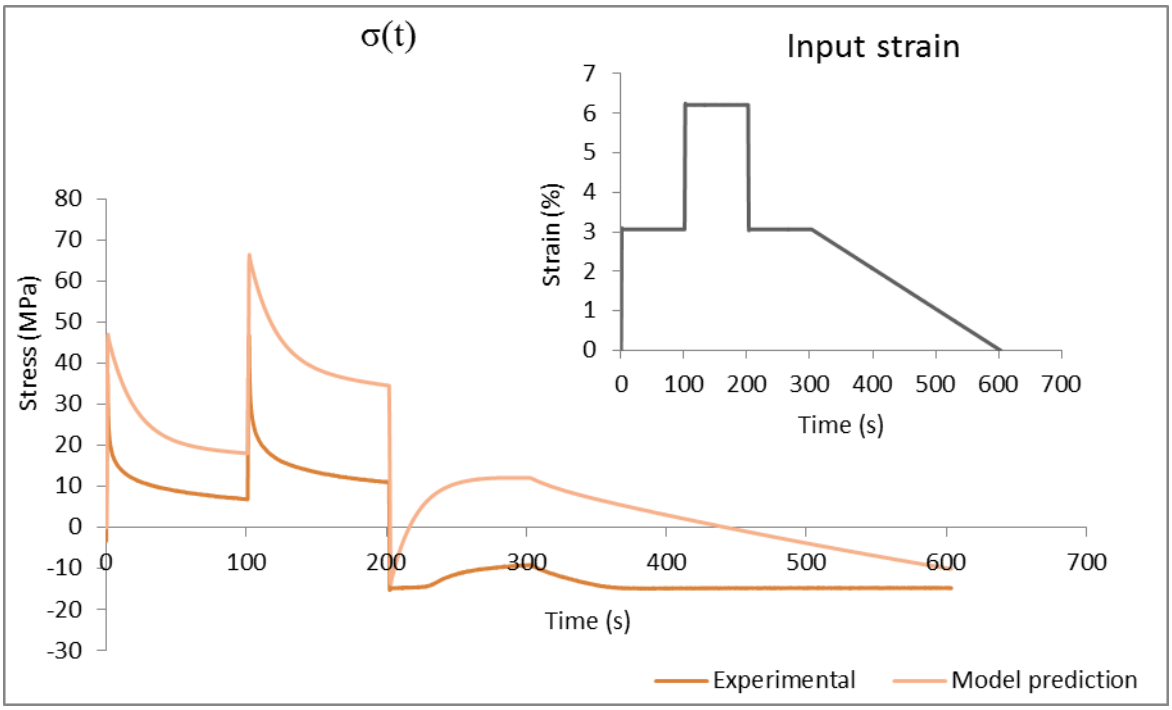

Figure 32 Burgers model best prediction of stress relaxation behaviour for cycle 1 data

- **Cycle 2**
  - Step 1: 8% $\varepsilon_{max.}$
  - Step 2: 4% $\varepsilon_{max.}$
  - Step 3: 8% $\varepsilon_{max.}$

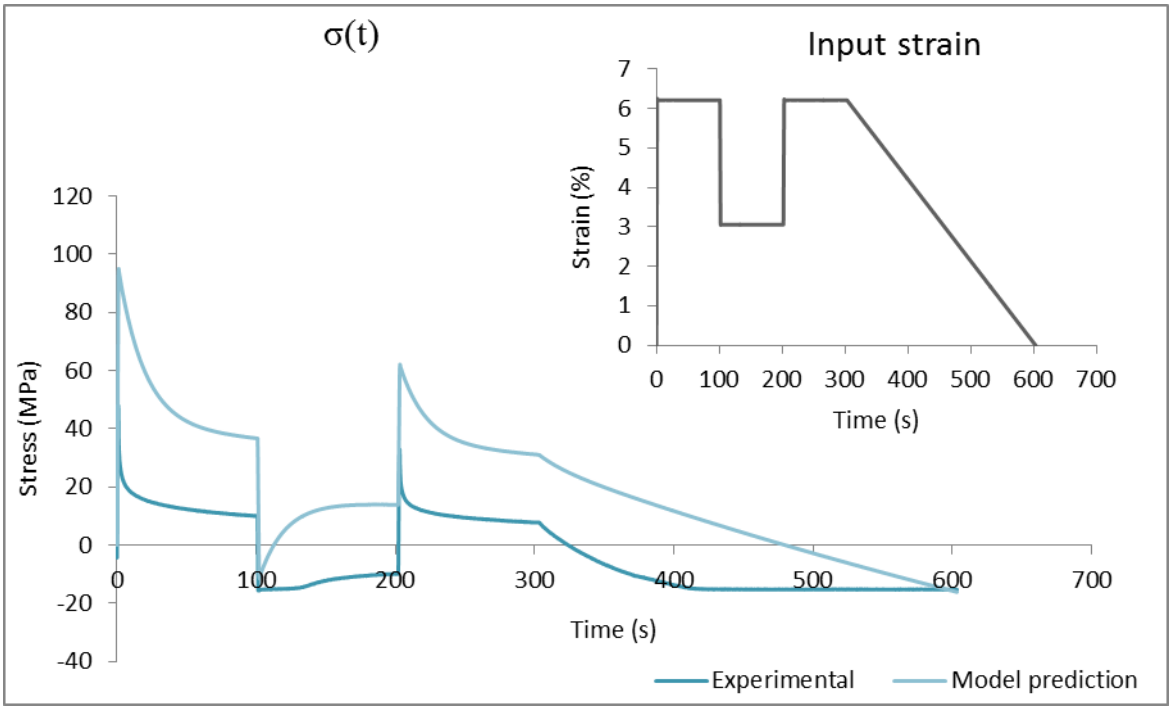

Figure 33 Burgers model best prediction of stress relaxation behaviour for cycle 2 data

- **Cycle 3**
  - Step 1: 4% $\varepsilon_{max.}$
  - Step 2: 8% $\varepsilon_{max.}$
  - Step 3: 12% $\varepsilon_{max.}$
  - Step 4: 16% $\varepsilon_{max.}$
  - Step 5: 12% $\varepsilon_{max.}$
  - Step 6: 8% $\varepsilon_{max.}$
  - Step 7: 4% $\varepsilon_{max.}$

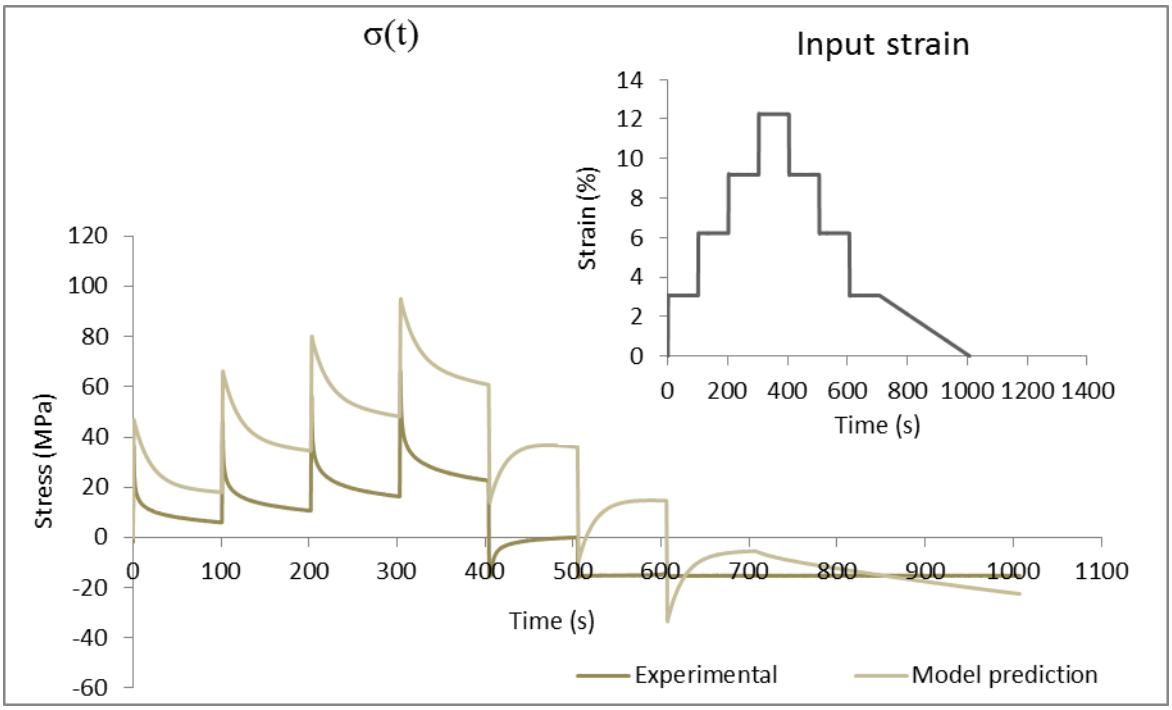

Figure 34 Burgers model best prediction of stress relaxation behaviour for cycle 3 data

Although model and experimental curves present a very similar behaviour, Figures 32-34 confirm that as the input strain increases so does the discrepancy between calculated and experimental values. The analysis of the same figures also confirms that the stress relaxation of PLA-PCL fibres assume negative values when strain changes from a higher step to a lower step.

4.2 Saturated specimens

Figure 35 intends to show that the fit of the model equation to the creep testing data of saturated specimens was not so satisfactory when compared with the adjustments obtained for dry specimens, even at the first level of input stress. This is because, as shown by the experimental curve, strains go well beyond 10%. For this analysis, other theories such as the large strain theory would be more appropriate. Still, when analysing the behaviour of the two curves, it is concluded that despite the coarse adjustment, the curve of the model can follow the trend experimental curve's behaviour.

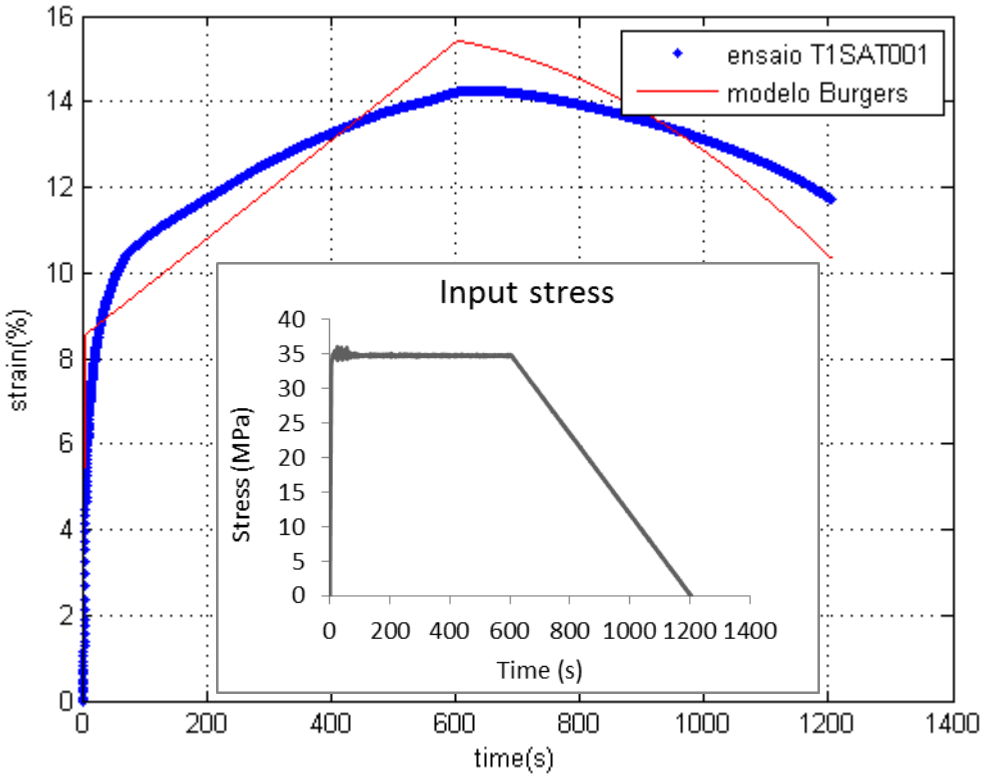

Figure 35 Best fit of the Burgers equation to the results obtained in the first creep level

Nevertheless, the Burgers parameters for this test of the first creep level are registered in Table 14.

Table 14 Burgers model parameters with 95% confidence bounds for T1_SAT_001 test

Test	R_1	St. Dev.	R_2	St. Dev.	η_1	St. Dev.	η_2	St. Dev.	R^2
T1_SAT_001	**36.27**	24.23	**4.537**	0.378	**3090**	12	**30.51**	5.56	0.7809

Based on these values, Figure 36 shows the best prediction of stress relaxation behaviour in the first level.

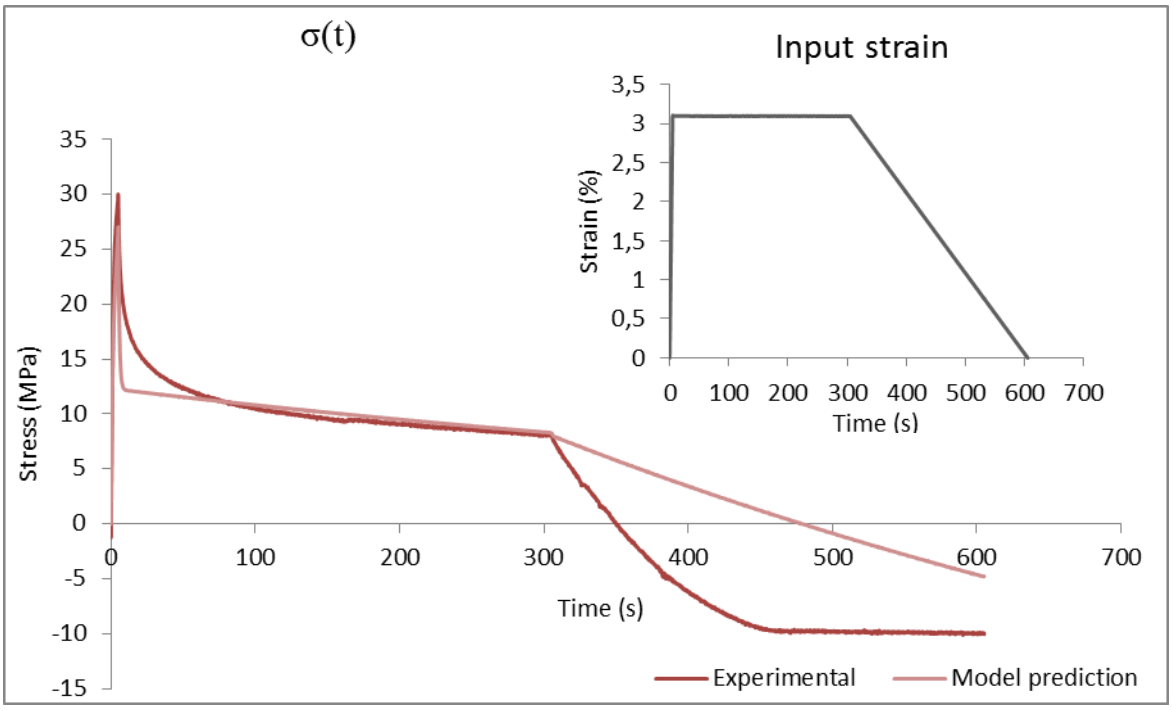

Figure 36 Burgers model best prediction of stress relaxation behaviour in the first level

The results of the experimental tests with saturation show that, although both curves do not present a similar behaviour as previously observed in tests without saturation, predicted and experimental values are now very close, particularly at the period between 100 and 300 seconds when the fibres are under constant strain. After the peak stress has been reached, the model predicts a more marked stress drop than what actually happens in the experimental curve. This sharp decrease may be related to the value of Kelvin viscosity (η_2) which is well less than the average value obtained for this same parameter from modelling the creep testing data with dry specimens (see Table 13). In order to confirm, a new modelling of the experimental results of this test (T1_SAT_001) was performed, now imposing the value of η_2 equal to the average obtained for the modelling results of the experimental data to dry fibres (η_2= 541.43). In this case, the Burgers equation has only 3 unknowns parameters (R_1, R_2 e η_1). The results of the new modelling are presented in Figure 37 and Table 15.

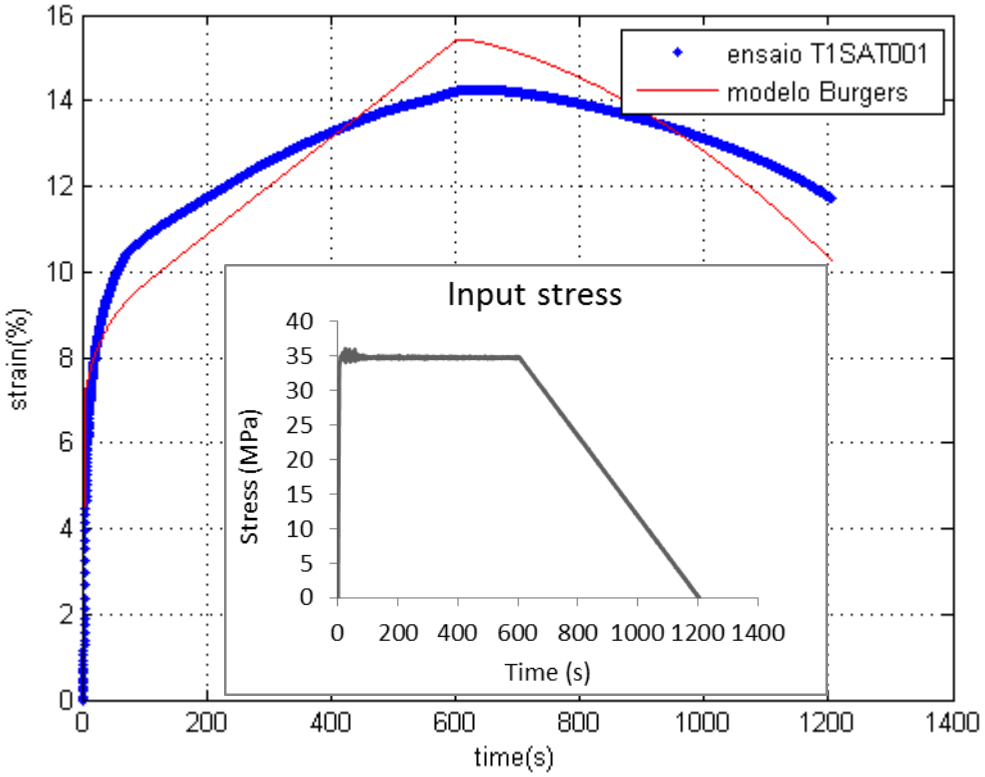

Figure 37 New fit of the Burgers equation to the results obtained in the first creep level (saturated specimens)

Table 15 Burgers model parameters with 95% confidence bounds for T1_SAT_001 test imposing η_2=541.43

Test	R_1	St. Dev.	R_2	St. Dev.	η_1	St. Dev.	R^2
T1_SAT_001	**4.975**	0.091	**21.6**	1.93	**3078**	14	0.7527

Looking at Figure 37 and the value of R^2 it follows that this new modelling is not better than the last one. However, with these new parameters, the model curve follows the experimental curve better during the increase in strain up to about 8% (compare Figures 35 and 37). In this initial phase, the most influential parameter for the creep behaviour is the elastic modulus (R_1), which suggests that this new value of 4.975 would be closer to the actual one than the value present in Table 14.

In Figure 38 the prediction of stress relaxation behaviour of PLA-PCL according the new Burgers parameters is presented.

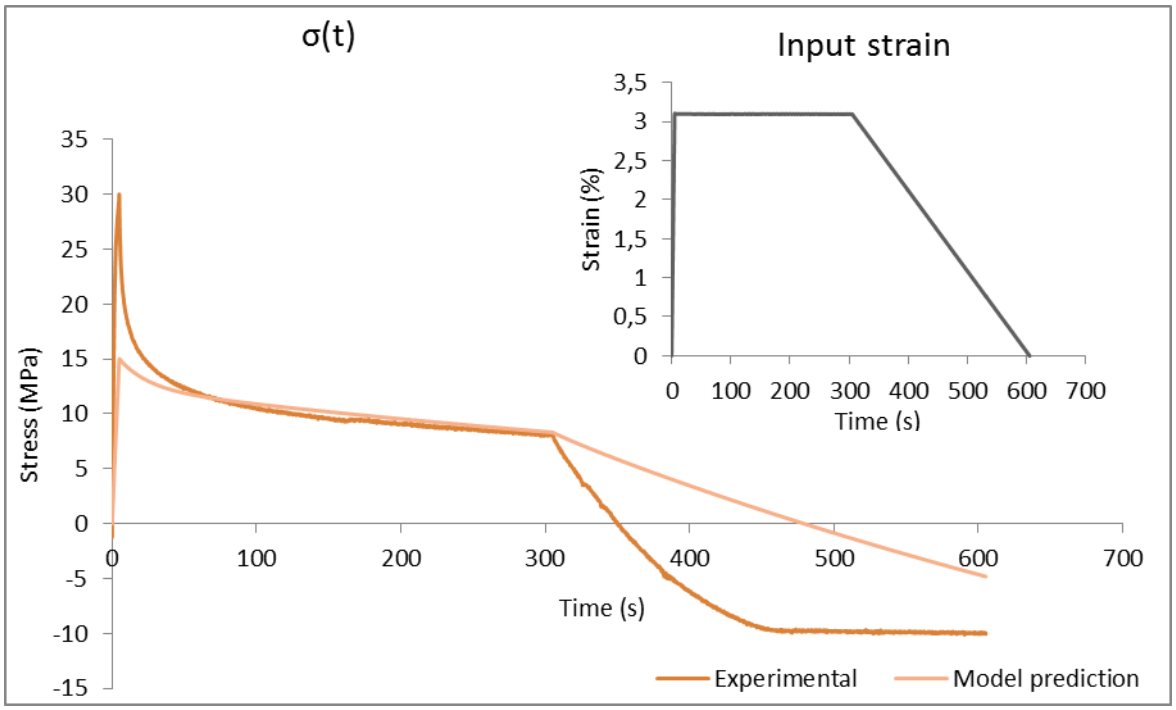

Figure 38 Burgers model new prediction of stress relaxation behaviour in the first level

The model curve has now a smoother transition from the peak stress to lower values. However, the maximum stress recorded in the mechanical test was about 30MPa whereas the model curve only reached the maximum of 15MPa (half of the actual value).

4.3 Conclusions

According to the modelling of creep testing data and knowing that the Burgers model is a linear viscoelastic model, the results indicate that the dry PLA-PCL fibres exhibit a linear behaviour under constant stress equal to or less than 35MPa. For higher creep levels, the Burgers' equation does not fit the experimental curve shape because the model is too simple and cannot predict the nonlinear behaviour of the material at high stress levels.

For the same input stress, of about 35MPa, saturated fibres appear to exhibit a nonlinear behaviour. This behaviour change, observed with saturation, is related with the strain values achieved that go well beyond 10%.

Still, despite the assumptions that were made, the linear viscoelastic model had some good results at predicting stress relaxation behaviour based on creep testing data, particularly in the first stress relaxation level.

5 Conclusions and Future Work

Natural ligament tissues display nonlinear viscoelastic behaviour and, during the developed work, evidence found proved that the biodegradable composite PLA-PCL exhibits the same kind of behaviour.

The results of tensile tests show some degradation in mechanical properties as a consequence of saturation. This analysis is important because, if implemented in a ligament device, this material will be subject to moisture (besides certain thermal and chemical conditions) typical of the human body. However, it should be reminded that in the scope of this project only fibres were tested, not a structure designed for ligament replacement. For this reason, the values obtained for the mechanical properties (Table 8) should not be directly compared with properties of the natural ligament.

From dynamic tests, the conclusions were that the rate of stress relaxation is strain dependent in PLA-PCL fibres, with the rate of relaxation decreasing as the strain level increases, and the rate of creep is stress dependent, with the rate of creep decreasing as the stress level increases. Provenzano et al. (2001) and Hingorani et al. (2003), with their studies in rat medial collateral ligament (MCL), reached the same conclusions about the rate of stress relaxation and the rate of creep for this ligament tissue [41, 42]. As future work, it is proposed the study of creep and stress relaxation behaviour of a human anterior cruciate ligament.

Still, in these creep and stress relaxation tests, the results suggest that saturation facilitates the deformation of the material and dry specimens show more pronounced stress relaxation than saturated specimens. In a future work, the same experimental tests should be repeated for specimens submitted to hydrolytic degradation process.

Lastly, the experimental data was submitted to a modelling process in order to understand if it was possible to predict the stress relaxation behaviour of this biocomposite material based on creep tests results. The model used was a simple linear viscoelastic model, the Burgers model (Figure 7), also known as the four element model.

The linear viscoelastic approach seems to be valid up to a certain stress level which is referred to as the linear viscoelastic threshold. Above this stress level the response of PLA-PCL becomes nonlinear. Considering the multiple creep levels it was observed that up to 35MPa a linear approach is still valid, while going up towards 71MPa a good fit to the experimental data cannot be achieved with the linear model. In the case of saturated fibres data, from the modelling results of the first creep level it can be concluded that a linear approach is not the most suitable one.

Nevertheless, the prediction of stress relaxation behaviour using the Burgers model may be considered qualitatively satisfactory, even for more complex cycles, although the model is simple and assumptions were made. The best results were obtained for the first stress relaxation level, where the input strain was about 3%.

Further studies should be done with other nonlinear and more complex models in order to achieve better modelling results. The Schapery single integral approach has been shown to be accurate and adaptable, and the modified superposition method (also commonly referred to as nonlinear superposition) allows the relaxation function to depend on strain. These models have been used for polymers and their formulations show potential for ligament mechanics [41].

ACKNOWLEDGMENTS

The support provided under the grant PTDC/EME-PME/114808/2009 by FCT (Portuguese Science and Technology Foundation) is acknowledged.

6 References

1. Surrao, D.C., S.D. Waldman, and B.G. Amsden, *Biomimetic poly(lactide) based fibrous scaffolds for ligament tissue engineering.* Acta Biomater, 2012. **8**(11): p. 3997-4006.
2. Fung, Y.C., *Biomechanics: Mechanical Properties of Living Tissue*. 1981, New Your: Springer-Verlag.
3. Sahoo, S., *An advanced biohybrid nano-microscaffold for tendon/ligament tissue engineering*, in *Division of Bioengineering*. 2008, National University of Singapore. p. 208.
4. Vieira, A.F.C., *Biomechanical Simulation Modelling of Biodegradable Composites in Ligament Tissue Augmentation Devices*, in *Faculty of Engineering*. 2011, University of Porto. p. 227.
5. Vieira, A.C., R.M. Guedes, and A.T. Marques, *Development of ligament tissue biodegradable devices: A review.* Journal of Biomechanics. **42**(15): p. 2421-2430.
6. Woo, S.L., et al., *Biomechanics of knee ligaments: injury, healing, and repair.* J Biomech, 2006. **39**(1): p. 1-20.
7. Laurencin, C.T. and J.W. Freeman, *Ligament tissue engineering: An evolutionary materials science approach.* Biomaterials, 2005. **26**(36): p. 7530-7536.
8. Vieira, A.C., et al., *Desenvolvimento de cordas biodegradáveis em PDO para regeneração de ligamentos*, in *Conferência Nacional de Biomecânica 2013*.
9. Rathbone, S. and S. Cartmell, *Tissue Engineering of Ligaments.*
10. Yilgor, C., P. Yilgor Huri, and G. Huri, *Tissue engineering strategies in ligament regeneration.* Stem Cells Int, 2012. **2012**: p. 374676.
11. Hampson, K., et al., *Tendon Tissue Engineering*, in *Tissue Engineering*, Eds. N Ashammakhi, R. Reis, and F.C. ©, Editors. 2008.
12. Kuo, C.K., J.E. Marturano, and R.S. Tuan, *Novel strategies in tendon and ligament tissue engineering: Advanced biomaterials and regeneration motifs.* Sports Med Arthrosc Rehabil Ther Technol, 2010. **2**(20): p. 1-14.
13. Sahoo, S., S.L. Toh, and J.C. Goh, *PLGA nanofiber-coated silk microfibrous scaffold for connective tissue engineering.* J Biomed Mater Res B Appl Biomater, 2010. **95**(1): p. 19-28.
14. Sell, S.A., et al., *The Use of Natural Polymers in Tissue Engineering: A Focus on Electrospun Extracellular Matrix Analogues.* Polymers, 2010. **2**(4): p. 522-553.
15. Vieira, A., et al., *Time-Dependent Damage on Biodegradable Devices.* Journal of Biomechanics, 2012. **45**: p. S59.
16. Spathis, G. and E. Kontou, *Creep failure time prediction of polymers and polymer composites.* Composites Science and Technology, 2012. **72**(9): p. 959-964.

17. Gautieri, A., et al., *Modeling and measuring visco-elastic properties: From collagen molecules to collagen fibrils.* International Journal of Non-Linear Mechanics, 2013. **56**: p. 25-33.

18. Holzapfel, G.A., *Nonlinear Solid Mechanics: A Continuum Approach for Engineering*. 2004: John Wiley & Sons, Ltd.

19. Jung, H.J., M.B. Fisher, and S.L. Woo, *Role of biomechanics in the understanding of normal, injured, and healing ligaments and tendons.* Sports Med Arthrosc Rehabil Ther Technol, 2009. **1**(1): p. 9.

20. Pena, E., J.A. Pena, and M. Doblare, *On modelling nonlinear viscoelastic effects in ligaments.* J Biomech, 2008. **41**(12): p. 2659-66.

21. Babacan, O., *Examining viscoelastic response of pregnant rat cervical using 3, 4, and 5 element spring and dashpot models*, in *Mechanical Engineering*. 2012, University of Illinois at Urbana-Champaign.

22. Robi, K., et al., *The Physiology of Sports Injuries and Repair Processes*, in *Current Issues in Sports and Exercise Medicine*. 2013.

23. Legnani, C., et al., *Anterior cruciate ligament reconstruction with synthetic grafts. A review of literature.* Int Orthop, 2010. **34**(4): p. 465-71.

24. Freeman, J.W. and A.L. Kwansa, *Recent Advancements in Ligament Tissue Engineering: The Use of Various Techniques and Materials for ACL Repair.* Recent Patents on Biomedical Engineering, 2008. **1**: p. 18-23.

25. Longo, U.G., et al., *Tendon augmentation grafts: a systematic review.* British Medical Bulletin, 2010. **94**(1): p. 165-188.

26. Nagarajan, S. and B. Reddy, *Bio-absorbable polyers in implantation: An overview.* Journal of Scientific & Industrial Research, 2009. **68**: p. 993-1009.

27. Yates, E.W., et al., *Ligament tissue engineering and its potential role in anterior cruciate ligament reconstruction.* Stem Cells Int, 2012. **2012**: 6 pages.

28. Cooper, J.A., et al., *Fiber-based tissue-engineered scaffold for ligament replacement: design considerations and in vitro evaluation.* Biomaterials, 2005. **26**(13): p. 1523-32.

29. Satyanarayana, K.G., G.G.C. Arizaga, and F. Wypych, *Biodegradable composites based on lignocellulosic fibers—An overview.* Progress in Polymer Science, 2009. **34**(9): p. 982-1021.

30. Araque-Monrós, M.C., et al., *Study of the degradation of a new PLA braided biomaterial in buffer phosphate saline, basic and acid media, intended for the regeneration of tendons and ligaments.* Polymer Degradation and Stability, 2013. **98**(9): p. 1563-1570.

31. Vroman, I. and L. Tighzert, *Biodegradable Polymers.* Materials, 2009. **2**: p. 307-344.

32. Ph.D. Tuzlakoglu, K. and R.L. Ph.D. Reis, *Biodegradable Polymeric Fiber Structures in Tissue Engineering.* TISSUE ENGINEERING, 2009. **15**(1): p. 17-27.

33. Lu, H.H., et al., *Anterior cruciate ligament regeneration using braided biodegradable scaffolds: in vitro optimization studies.* Biomaterials, 2005. **26**(23): p. 4805-16.

34. Sahoo, S., et al., *Characterization of a Novel Polymeric Scaffold for Potential Application in Tendon/Ligament Tissue Engineering.* TISSUE ENGINEERING, 2006. **12**.

35. Vieira, A.C., et al., *Biomechanics of biomaterials used in soft tissue regenerative medicine*, in *XXXI Simposio de la Sociedad Ibérica de Biomecánica y Biomateriales*, Biomecánica, Editor. 2009. p. 7-14.

36. Findley, W.N., *Creep and relaxation of nonlinear viscoelastic materials (with an Introduction to Linear Viscoelasticity)*. 1976, New York: Dover Publisher, INC.

37. Jia, Y., et al., *Creep and recovery of polypropylene/carbon nanotube composites.* International Journal of Plasticity, 2011. **27**(8): p. 1239-1251.

38. Liu, X., et al., *Study on the creep and recovery behaviors of UHMWPE/CNTs composite fiber*. Fibers and Polymers, 2013. **14**(10): p. 1635-1640.

39. Brinson, H. and L. Brinson, *Polymer Engineering Science and Viscoelasticity - An Introduction*. 2008, New York: Springer. 446.

40. Dey, A. and P. Basudhar, *Applicability of Burger Model in Predicting the Response of Viscoelastic Soil Beds.* GeoFlorida 2010: Advances in Analysis, Modeling & Design, 2010: p. 2611-2620.

41. Provenzano, P.P., et al., *Application of nonlinear viscoelastic models to describe ligament behavior.* Biomech Model Mechanobiol, 2002. **1**(1): p. 45-57.

42. Hingorani, R.V., et al., *Nonlinear Viscoelasticity in Rabbit Medial Collateral Ligament.* Annals of Biomedical Engineering, 2003. **32(**2): p. 306–312.

ANNEX A: Experimental Data

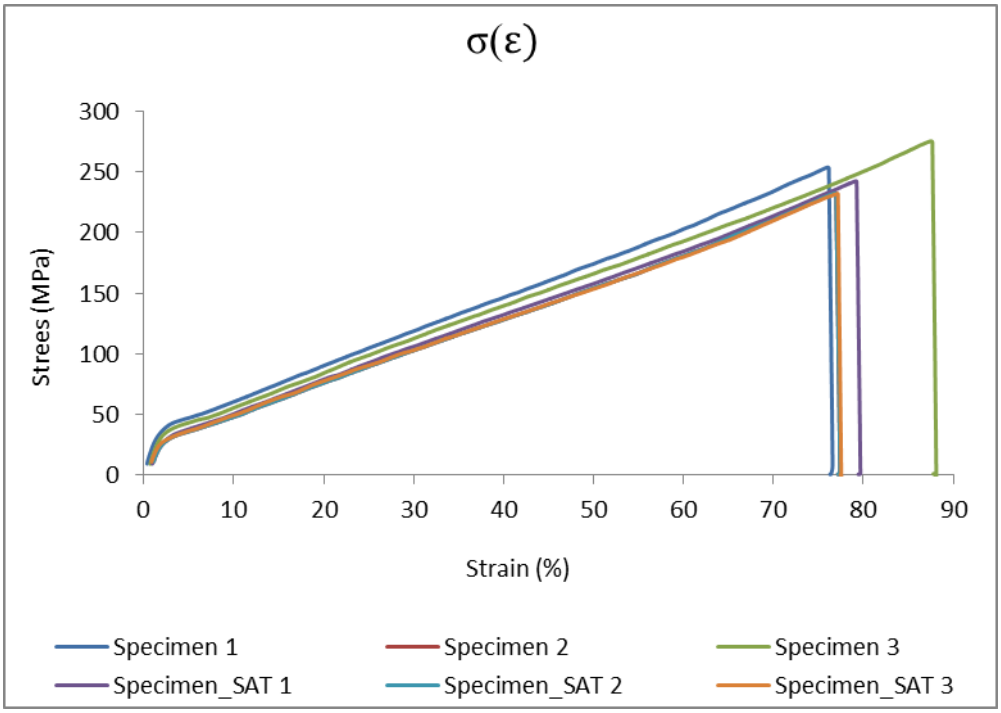

Figure 39 Results of the tensile tests

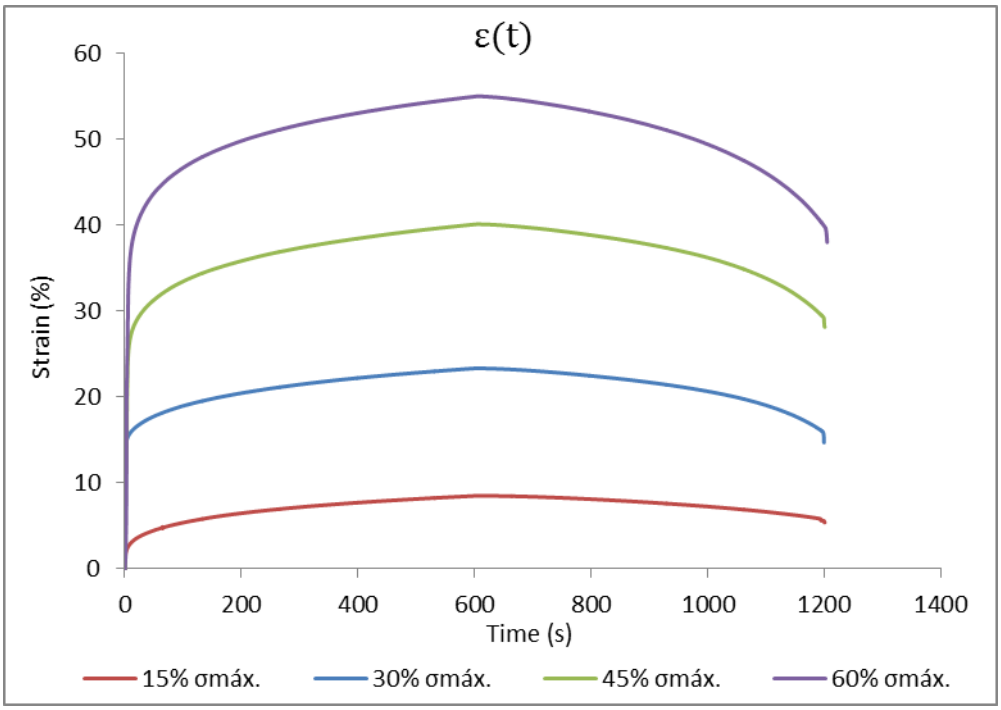

Figure 40 Creep behaviour at multiple levels of stress – 3 specimens's data average (dry specimens)

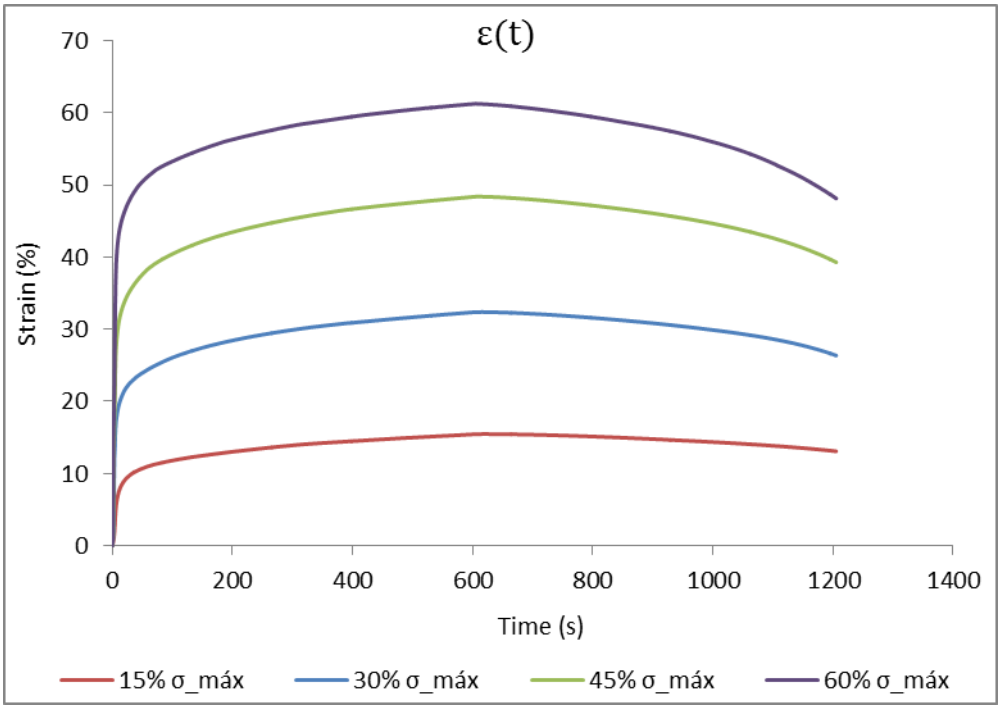

Figure 41 Creep behaviour at multiple levels of stress – 3 specimens' data average (saturated specimens)

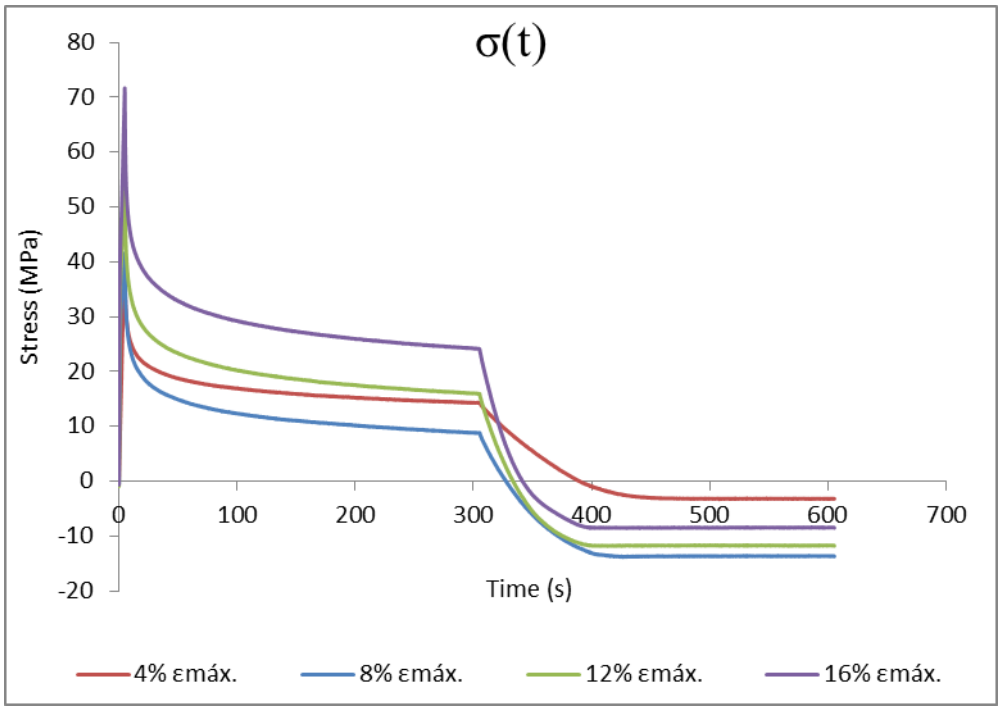

Figure 42 Stress relaxation behaviour at multiple levels of strain – 3 specimens' data average (dry specimens)

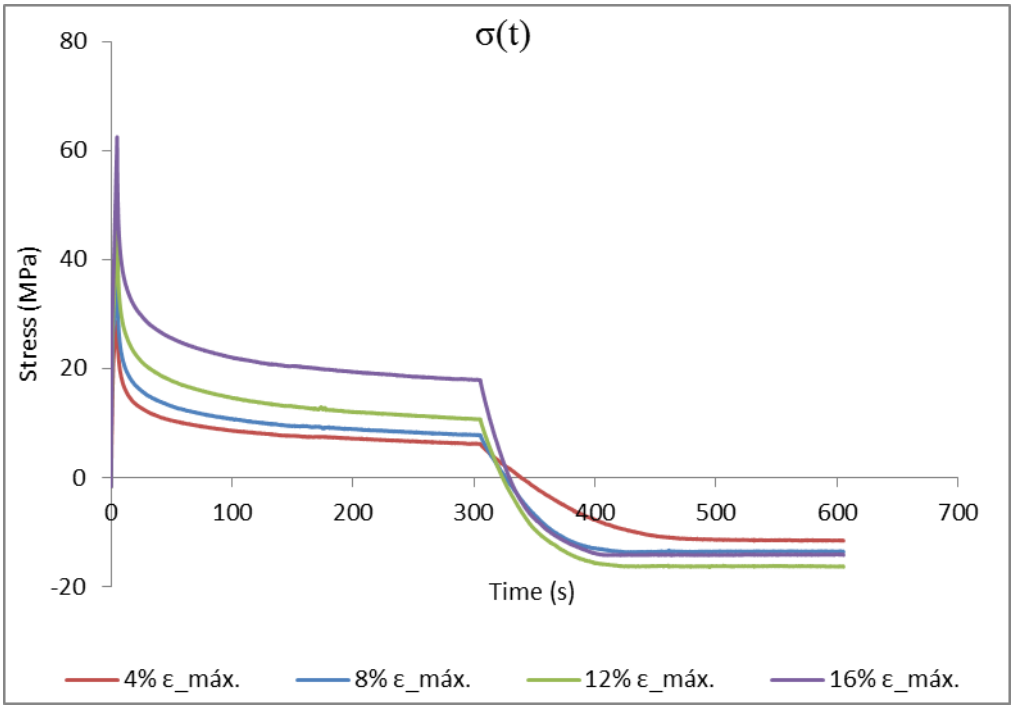

Figure 43 Stress relaxation behaviour at multiple levels of strain – 3 specimens' data average (saturated specimens)

ANNEX B: Burgers model equation

Modelo de Burgers

```
> restart:
> unassign('R1','R2','n1','n2','ds0','s0'):
> eq:=sigma(t)+(n1/R1+n1/R2+n2/R2)*diff(sigma(t),t)+n1*n2/R1/R2*di
  ff(sigma(t),t$2)-n1*diff(epsilon(t),t)-n1*n2/R2*diff(epsilon(t),
  t$2);
```

$$eq := \sigma(t) + \left(\frac{n1}{R1} + \frac{n1}{R2} + \frac{n2}{R2}\right)\left(\frac{d}{dt}\sigma(t)\right) + \frac{n1\,n2\left(\frac{d^2}{dt^2}\sigma(t)\right)}{R1\,R2} - n1\left(\frac{d}{dt}\varepsilon(t)\right) - \frac{n1\,n2\left(\frac{d^2}{dt^2}\varepsilon(t)\right)}{R2}$$

CONSTANT STRESS RATE

```
> ode:=subs(sigma(t)=ds0*t*Heaviside(t),eq);
```

$$ode := ds0\,t\,\text{Heaviside}(t) + \left(\frac{n1}{R1} + \frac{n1}{R2} + \frac{n2}{R2}\right)\left(\frac{\partial}{\partial t}(ds0\,t\,\text{Heaviside}(t))\right) + \frac{n1\,n2\left(\frac{\partial^2}{\partial t^2}(ds0\,t\,\text{Heaviside}(t))\right)}{R1\,R2} - n1\left(\frac{d}{dt}\varepsilon(t)\right) - \frac{n1\,n2\left(\frac{d^2}{dt^2}\varepsilon(t)\right)}{R2}$$

```
> sol1:=dsolve( {ode, epsilon(0)=0, D(epsilon)(0)=ds0/R1},
  epsilon(t));
```

$$sol1 := \varepsilon(t) = \frac{1}{2}\frac{ds0\,\text{Heaviside}(t)\,t^2}{n1} + \frac{ds0\,t\,\text{Heaviside}(t)}{R1} + \frac{ds0\,t\,\text{Heaviside}(t)}{R2} + \frac{ds0\,\text{Heaviside}(t)\,\mathbf{e}^{\left(-\frac{R2\,t}{n2}\right)}\,n2}{R2^2} - \frac{ds0\,\text{Heaviside}(t)\,n2}{R2^2}$$

```
> sol1a:=expand(subs(Heaviside(t)=1,sol1));
```

$$sol1a := \varepsilon(t) = \frac{ds0\,t^2}{2\,n1} + \frac{ds0\,t}{R1} + \frac{ds0\,t}{R2} + \frac{ds0\,n2}{R2^2\,\mathbf{e}^{\left(\frac{R2\,t}{n2}\right)}} - \frac{ds0\,n2}{R2^2}$$

RAMP LOAD

```
> stress:=s0/t1*t*Heaviside(t)-s0/t1*(t-t1)*Heaviside(t-t1)-s0/(t3
  -t2)*(t-t2)*Heaviside(t-t2)+s0/(t3-t2)*(t-t3)*Heaviside(t-t3);
```

$$stress := \frac{s0\,t\,\text{Heaviside}(t)}{t1} - \frac{s0\,(t-t1)\,\text{Heaviside}(t-t1)}{t1} - \frac{s0\,(t-t2)\,\text{Heaviside}(t-t2)}{t3-t2} + \frac{s0\,(t-t3)\,\text{Heaviside}(t-t3)}{t3-t2}$$

exemplo

```
> plot(subs(t1=1,t2=10,t3=16,s0=1,stress),t=0..40);
```

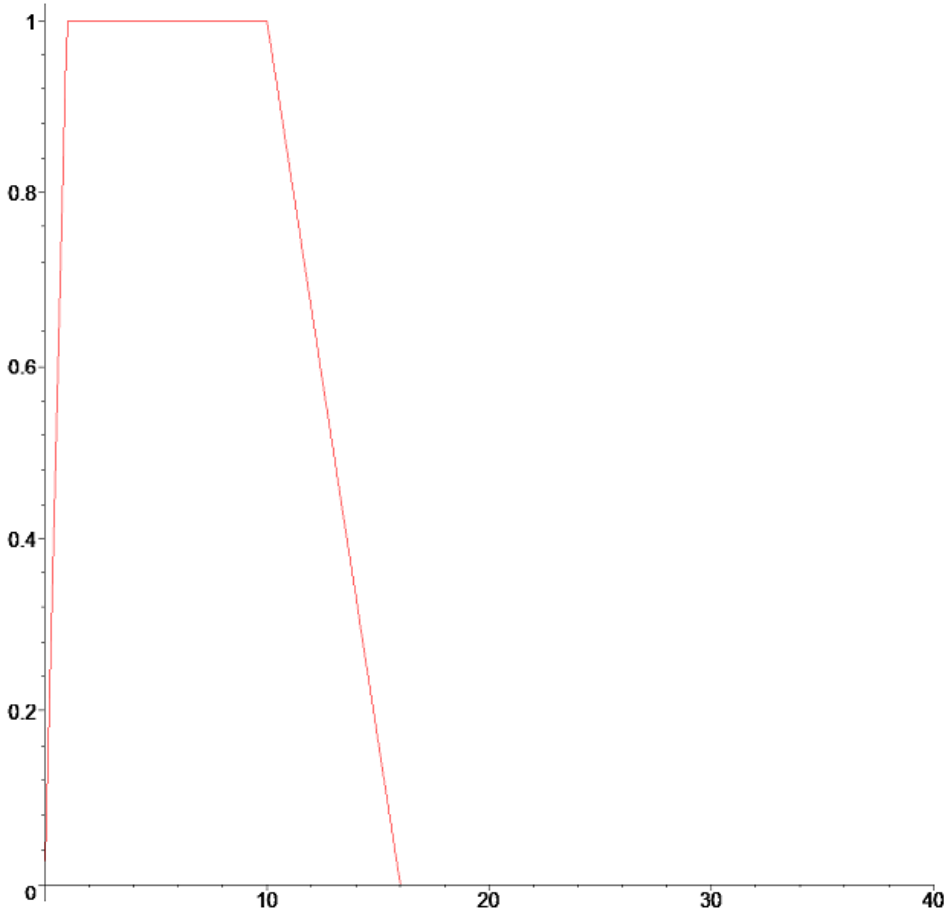


```
> strain:=subs(ds0=s0/t1,rhs(sol1a))*Heaviside(t)-subs(ds0=s0/t1,t
  =t-t1,rhs(sol1a))*Heaviside(t-t1)-subs(ds0=s0/(t3-t2),t=t-t2,rhs
  (sol1a))*Heaviside(t-t2)+subs(ds0=s0/(t3-t2),t=t-t3,rhs(sol1a))*
  Heaviside(t-t3);
```

$$strain := \left(\frac{s0\,t^2}{2\,n1\,t1} + \frac{s0\,t}{R1\,t1} + \frac{s0\,t}{R2\,t1} + \frac{s0\,n2}{R2^2\,t1\,\mathbf{e}^{\left(\frac{R2\,t}{n2}\right)}} - \frac{s0\,n2}{R2^2\,t1} \right) \mathrm{Heaviside}(t)$$

$$- \left(\frac{s0\,(t-t1)^2}{2\,n1\,t1} + \frac{s0\,(t-t1)}{R1\,t1} + \frac{s0\,(t-t1)}{R2\,t1} + \frac{s0\,n2}{R2^2\,t1\,\mathbf{e}^{\left(\frac{R2\,(t-t1)}{n2}\right)}} - \frac{s0\,n2}{R2^2\,t1} \right) \mathrm{Heaviside}(t-t1)$$

$$-\left(\frac{s0\,(t-t2)^2}{2\,n1\,(t3-t2)}+\frac{s0\,(t-t2)}{R1\,(t3-t2)}+\frac{s0\,(t-t2)}{R2\,(t3-t2)}+\frac{s0\,n2}{R2^2\,(t3-t2)\,\mathbf{e}^{\left(\frac{R2\,(t-t2)}{n2}\right)}}-\frac{s0\,n2}{R2^2\,(t3-t2)}\right)$$

$$\text{Heaviside}(t-t2)+$$

$$\left(\frac{s0\,(t-t3)^2}{2\,n1\,(t3-t2)}+\frac{s0\,(t-t3)}{R1\,(t3-t2)}+\frac{s0\,(t-t3)}{R2\,(t3-t2)}+\frac{s0\,n2}{R2^2\,(t3-t2)\,\mathbf{e}^{\left(\frac{R2\,(t-t3)}{n2}\right)}}-\frac{s0\,n2}{R2^2\,(t3-t2)}\right)$$

$$\text{Heaviside}(t-t3)$$

```
> #assume(t3>t2,t2>t1,t1>0);convert(strain,piecewise,t);
```

exemplo

```
> plot(subs(R1=1,R2=1,n1=100,n2=1,s0=1,t1=1,t2=10,t3=16,s0=1,strai
  n),t=0..30);
```

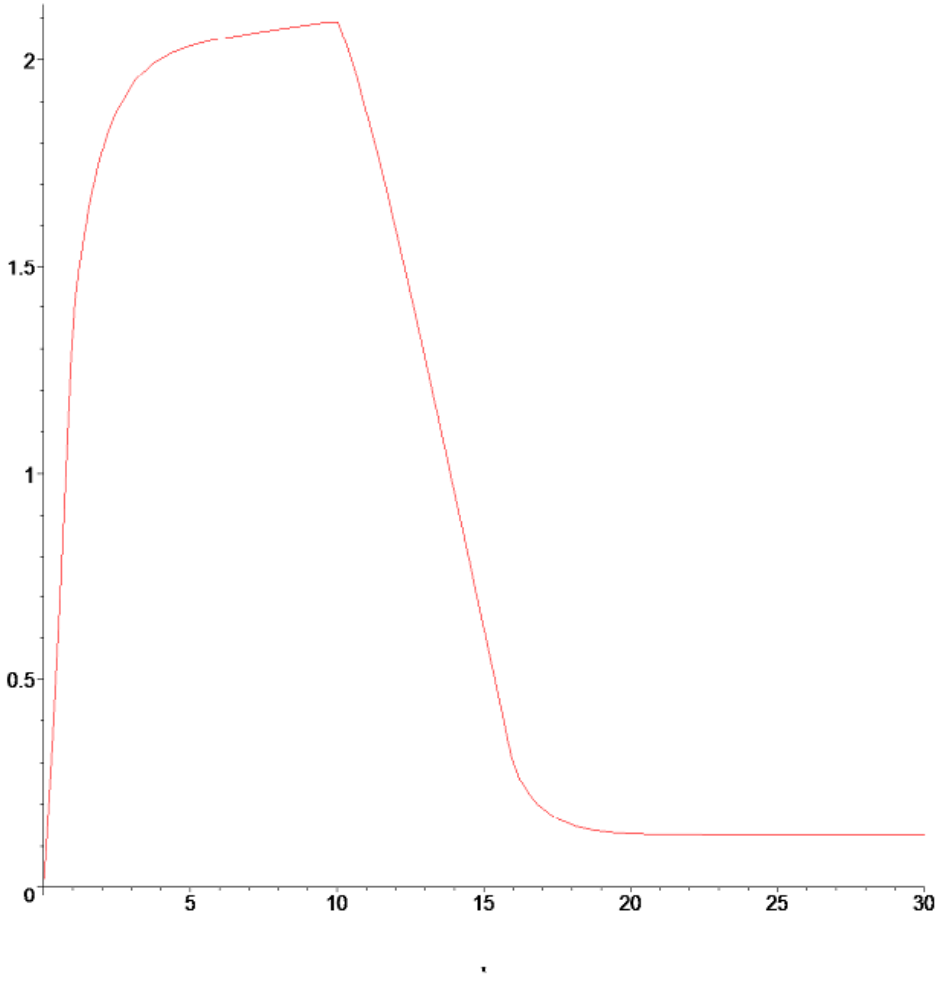

Burgers equation:

f(t)=(1/2/n1*s0/t1*t^2+1/R1*s0/t1*t+1/R2*s0/t1*t+1/R2^2*s0/t1/exp(1/n2*R2*t)*n2-1/R2^2*s0/t1*n2)*heaviside(t)-(1/2/n1*s0/t1*(t-t1)^2+1/R1*s0/t1*(t-t1)+1/R2*s0/t1*(t-t1)+1/R2^2*s0/t1/exp(1/n2*R2*(t-t1))*n2-1/R2^2*s0/t1*n2)*heaviside(t-t1)-(1/2/n1*s0/(t3-t2)*(t-t2)^2+1/R1*s0/(t3-t2)*(t-t2)+1/R2*s0/(t3-t2)*(t-t2)+1/R2^2*s0/(t3-t2)/exp(1/n2*R2*(t-t2))*n2-1/R2^2*s0/(t3-t2)*n2)*heaviside(t-t2)+(1/2/n1*s0/(t3-t2)*(t-t3)^2+1/R1*s0/(t3-t2)*(t-t3)+1/R2*s0/(t3-t2)*(t-t3)+1/R2^2*s0/(t3-t2)/exp(1/n2*R2*(t-t3))*n2-1/R2^2*s0/(t3-t2)*n2)*heaviside(t-t3)

Level 1: 15%smax.

(tests T1_00*): t1=1.2s; t2=601.2s; t3=1201.2s; s0=35.663

f(t)=(1/2/n1*35.663/1.2*x^2+1/R1*35.663/1.2*x+1/R2*35.663/1.2*x+1/R2^2*35.663/1.2/exp(1/n2*R2*x)*n2-1/R2^2*35.663/1.2*n2)*heaviside(t)-(1/2/n1*35.663/1.2*(x-1.2)^2+1/R1*35.663/1.2*(x-1.2)+1/R2*35.663/1.2*(x-1.2)+1/R2^2*35.663/1.2/exp(1/n2*R2*(x-1.2))*n2-1/R2^2*35.663/1.2*n2)*heaviside(t-1.2)-(1/2/n1*35.663/(1201.2-601.2)*(x-601.2)^2+1/R1*35.663/(1201.2-601.2)*(x-601.2)+1/R2*35.663/(1201.2-601.2)*(x-601.2)+1/R2^2*35.663/(1201.2-601.2)/exp(1/n2*R2*(x-601.2))*n2-1/R2^2*35.663/(1201.2-601.2)*n2)*heaviside(t-601.2)+(1/2/n1*35.663/(1201.2-601.2)*(x-1201.2)^2+1/R1*35.663/(1201.2-601.2)*(x-1201.2)+1/R2*35.663/(1201.2-601.2)*(x-1201.2)+1/R2^2*35.663/(1201.2-601.2)/exp(1/n2*R2*(x-1201.2))*n2-1/R2^2*35.663/(1201.2-601.2)*n2)*heaviside(t-1201.2)

(tests T1_SAT_00*): t1=5.2s; t2=605.2s; t3=1205.2s; s0=34.833

f(t)=(1/2/n1*34.833/5.2*x^2+1/R1*34.833/5.2*x+1/R2*34.833/5.2*x+1/R2^2*34.833/5.2/exp(1/n2*R2*x)*n2-1/R2^2*34.833/5.2*n2)*heaviside(t)-(1/2/n1*34.833/5.2*(x-5.2)^2+1/R1*34.833/5.2*(x-5.2)+1/R2*34.833/5.2*(x-5.2)+1/R2^2*34.833/5.2/exp(1/n2*R2*(x-5.2))*n2-1/R2^2*34.833/5.2*n2)*heaviside(t-5.2)-(1/2/n1*34.833/(1205.2-605.2)*(x-605.2)^2+1/R1*34.833/(1205.2-605.2)*(x-605.2)+1/R2*34.833/(1205.2-605.2)*(x-605.2)+1/R2^2*34.833/(1205.2-605.2)/exp(1/n2*R2*(x-605.2))*n2-1/R2^2*34.833/(1205.2-605.2)*n2)*heaviside(t-605.2)+(1/2/n1*34.833/(1205.2-605.2)*(x-1205.2)^2+1/R1*34.833/(1205.2-605.2)*(x-1205.2)+1/R2*34.833/(1205.2-605.2)*(x-1205.2)+1/R2^2*34.833/(1205.2-605.2)/exp(1/n2*R2*(x-1205.2))*n2-1/R2^2*34.833/(1205.2-605.2)*n2)*heaviside(t-1205.2)

(tests T1_SAT_001): Imposing n2=543.41

f(t)=(1/2/n1*34.833/5.2*x^2+1/R1*34.833/5.2*x+1/R2*34.833/5.2*x+1/R2^2*34.833/5.2/exp(1/543.41*R2*x)*543.41-1/R2^2*34.833/5.2*543.41)*heaviside(t)-(1/2/n1*34.833/5.2*(x-5.2)^2+1/R1*34.833/5.2*(x-5.2)+1/R2*34.833/5.2*(x-5.2)+1/R2^2*34.833/5.2/exp(1/543.41*R2*(x-5.2))*543.41-1/R2^2*34.833/5.2*543.41)*heaviside(t-5.2)-(1/2/n1*34.833/(1205.2-605.2)*(x-605.2)^2+1/R1*34.833/(1205.2-605.2)*(x-605.2)+1/R2*34.833/(1205.2-605.2)*(x-605.2)+1/R2^2*34.833/(1205.2-605.2)/exp(1/543.41*R2*(x-605.2))*543.41-1/R2^2*34.833/(1205.2-605.2)*543.41)*heaviside(t-605.2)+(1/2/n1*34.833/(1205.2-605.2)*(x-1205.2)^2+1/R1*34.833/(1205.2-605.2)*(x-1205.2)+1/R2*34.833/(1205.2-

605.2)*(x-1205.2)+1/R2^2*34.833/(1205.2-605.2)/exp(1/543.41*R2*(x-1205.2))*543.41-1/R2^2*34.833/(1205.2-605.2)*543.41)*heaviside(t-1205.2)

Level 2: 30%smax.

(tests T2_00*): t1=1.2s; t2=601.2s; t3=1201.2s; s0=71.325

f(t)=(1/2/n1*71.325/1.2*x^2+1/R1*71.325/1.2*x+1/R2*71.325/1.2*x+1/R2^2*71.325/1.2/exp(1/n2*R2*x)*n2-1/R2^2*71.325/1.2*n2)*heaviside(t)-(1/2/n1*71.325/1.2*(x-1.2)^2+1/R1*71.325/1.2*(x-1.2)+1/R2*71.325/1.2*(x-1.2)+1/R2^2*71.325/1.2/exp(1/n2*R2*(x-1.2))*n2-1/R2^2*71.325/1.2*n2)*heaviside(t-1.2)-(1/2/n1*71.325/(1201.2-601.2)*(x-601.2)^2+1/R1*71.325/(1201.2-601.2)*(x-601.2)+1/R2*71.325/(1201.2-601.2)*(x-601.2)+1/R2^2*71.325/(1201.2-601.2)/exp(1/n2*R2*(x-601.2))*n2-1/R2^2*71.325/(1201.2-601.2)*n2)*heaviside(t-601.2)+(1/2/n1*71.325/(1201.2-601.2)*(x-1201.2)^2+1/R1*71.325/(1201.2-601.2)*(x-1201.2)+1/R2*71.325/(1201.2-601.2)*(x-1201.2)+1/R2^2*71.325/(1201.2-601.2)/exp(1/n2*R2*(x-1201.2))*n2-1/R2^2*71.325/(1201.2-601.2)*n2)*heaviside(t-1201.2)

(tests T2_SAT_00*): t1=5.2s; t2=605.2s; t3=1205.2s; s0=69.666

f(t)=(1/2/n1*69.666/5.2*x^2+1/R1*69.666/5.2*x+1/R2*69.666/5.2*x+1/R2^2*69.666/5.2/exp(1/n2*R2*x)*n2-1/R2^2*69.666/5.2*n2)*heaviside(t)-(1/2/n1*69.666/5.2*(x-5.2)^2+1/R1*69.666/5.2*(x-5.2)+1/R2*69.666/5.2*(x-5.2)+1/R2^2*69.666/5.2/exp(1/n2*R2*(x-5.2))*n2-1/R2^2*69.666/5.2*n2)*heaviside(t-5.2)-(1/2/n1*69.666/(1205.2-605.2)*(x-605.2)^2+1/R1*69.666/(1205.2-605.2)*(x-605.2)+1/R2*69.666/(1205.2-605.2)*(x-605.2)+1/R2^2*69.666/(1205.2-605.2)/exp(1/n2*R2*(x-605.2))*n2-1/R2^2*69.666/(1205.2-605.2)*n2)*heaviside(t-605.2)+(1/2/n1*69.666/(1205.2-605.2)*(x-1205.2)^2+1/R1*69.666/(1205.2-605.2)*(x-1205.2)+1/R2*69.666/(1205.2-605.2)*(x-1205.2)+1/R2^2*69.666/(1205.2-605.2)/exp(1/n2*R2*(x-1205.2))*n2-1/R2^2*69.666/(1205.2-605.2)*n2)*heaviside(t-1205.2)

Level 3: 45%smax.

(tests T3_00*): t1=1.2s; t2=601.2s; t3=1201.2s; s0=106.99

f(t)=(1/2/n1*106.99/1.2*x^2+1/R1*106.99/1.2*x+1/R2*106.99/1.2*x+1/R2^2*106.99/1.2/exp(1/n2*R2*x)*n2-1/R2^2*106.99/1.2*n2)*heaviside(t)-(1/2/n1*106.99/1.2*(x-1.2)^2+1/R1*106.99/1.2*(x-1.2)+1/R2*106.99/1.2*(x-1.2)+1/R2^2*106.99/1.2/exp(1/n2*R2*(x-1.2))*n2-1/R2^2*106.99/1.2*n2)*heaviside(t-1.2)-(1/2/n1*106.99/(1201.2-601.2)*(x-601.2)^2+1/R1*106.99/(1201.2-601.2)*(x-601.2)+1/R2*106.99/(1201.2-601.2)*(x-601.2)+1/R2^2*106.99/(1201.2-601.2)/exp(1/n2*R2*(x-601.2))*n2-1/R2^2*106.99/(1201.2-601.2)*n2)*heaviside(t-601.2)+(1/2/n1*106.99/(1201.2-601.2)*(x-1201.2)^2+1/R1*106.99/(1201.2-601.2)*(x-1201.2)+1/R2*106.99/(1201.2-601.2)*(x-1201.2)+1/R2^2*106.99/(1201.2-601.2)/exp(1/n2*R2*(x-1201.2))*n2-1/R2^2*106.99/(1201.2-601.2)*n2)*heaviside(t-1201.2)

(tests T3_SAT_00*): t1=5.2s; t2=605.2s; t3=1205.2s; s0=104.50

f(t)=(1/2/n1*104.50/5.2*x^2+1/R1*104.50/5.2*x+1/R2*104.50/5.2*x+1/R2^2*104.50/5.2/exp(1/n2*R2*x)*n2-1/R2^2*104.50/5.2*n2)*heaviside(t)-(1/2/n1*104.50/5.2*(x-5.2)^2+1/R1*104.50/5.2*(x-5.2)+1/R2*104.50/5.2*(x-5.2)+1/R2^2*104.50/5.2/exp(1/n2*R2*(x-5.2))*n2-1/R2^2*104.50/5.2*n2)*heaviside(t-5.2)-(1/2/n1*104.50/(1205.2-605.2)*(x-605.2)^2+1/R1*104.50/(1205.2-605.2)*(x-605.2)+1/R2*104.50/(1205.2-605.2)*(x-605.2)+1/R2^2*104.50/(1205.2-605.2)/exp(1/n2*R2*(x-605.2))*n2-1/R2^2*104.50/(1205.2-605.2)*n2)*heaviside(t-605.2)+(1/2/n1*104.50/(1205.2-605.2)*(x-1205.2)^2+1/R1*104.50/(1205.2-605.2)*(x-1205.2)+1/R2*104.50/(1205.2-605.2)*(x-1205.2)+1/R2^2*104.50/(1205.2-605.2)/exp(1/n2*R2*(x-1205.2))*n2-1/R2^2*104.50/(1205.2-605.2)*n2)*heaviside(t-1205.2)

Level 4: 60%smax.

(tests T4_00*): t1=1.2s; t2=601.2s; t3=1201.2s; s0=142.65

f(t)=(1/2/n1*142.65/1.2*x^2+1/R1*142.65/1.2*x+1/R2*142.65/1.2*x+1/R2^2*142.65/1.2/exp(1/n2*R2*x)*n2-1/R2^2*142.65/1.2*n2)*heaviside(t)-(1/2/n1*142.65/1.2*(x-1.2)^2+1/R1*142.65/1.2*(x-1.2)+1/R2*142.65/1.2*(x-1.2)+1/R2^2*142.65/1.2/exp(1/n2*R2*(x-1.2))*n2-1/R2^2*142.65/1.2*n2)*heaviside(t-1.2)-(1/2/n1*142.65/(1201.2-601.2)*(x-601.2)^2+1/R1*142.65/(1201.2-601.2)*(x-601.2)+1/R2*142.65/(1201.2-601.2)*(x-601.2)+1/R2^2*142.65/(1201.2-601.2)/exp(1/n2*R2*(x-601.2))*n2-1/R2^2*142.65/(1201.2-601.2)*n2)*heaviside(t-601.2)+(1/2/n1*142.65/(1201.2-601.2)*(x-1201.2)^2+1/R1*142.65/(1201.2-601.2)*(x-1201.2)+1/R2*142.65/(1201.2-601.2)*(x-1201.2)+1/R2^2*142.65/(1201.2-601.2)/exp(1/n2*R2*(x-1201.2))*n2-1/R2^2*142.65/(1201.2-601.2)*n2)*heaviside(t-1201.2)

(tests T4_SAT_00*): t1=5.2s; t2=605.2s; t3=1205.2s; s0=139.33

f(t)=(1/2/n1*139.33/5.2*x^2+1/R1*139.33/5.2*x+1/R2*139.33/5.2*x+1/R2^2*139.33/5.2/exp(1/n2*R2*x)*n2-1/R2^2*139.33/5.2*n2)*heaviside(t)-(1/2/n1*139.33/5.2*(x-5.2)^2+1/R1*139.33/5.2*(x-5.2)+1/R2*139.33/5.2*(x-5.2)+1/R2^2*139.33/5.2/exp(1/n2*R2*(x-5.2))*n2-1/R2^2*139.33/5.2*n2)*heaviside(t-5.2)-(1/2/n1*139.33/(1205.2-605.2)*(x-605.2)^2+1/R1*139.33/(1205.2-605.2)*(x-605.2)+1/R2*139.33/(1205.2-605.2)*(x-605.2)+1/R2^2*139.33/(1205.2-605.2)/exp(1/n2*R2*(x-605.2))*n2-1/R2^2*139.33/(1205.2-605.2)*n2)*heaviside(t-605.2)+(1/2/n1*139.33/(1205.2-605.2)*(x-1205.2)^2+1/R1*139.33/(1205.2-605.2)*(x-1205.2)+1/R2*139.33/(1205.2-605.2)*(x-1205.2)+1/R2^2*139.33/(1205.2-605.2)/exp(1/n2*R2*(x-1205.2))*n2-1/R2^2*139.33/(1205.2-605.2)*n2)*heaviside(t-1205.2)

ANNEX C: Matlab programs

ProcessData

```
% Os ficheiros com extensao xlsx respeitantes aos resultados experimentais
% sao importados e, para cada ficheiro, e gerada uma matriz com as coluna
% correspondentes as diferentes grandezas medidas durante o ensaio
% experimental e que se encontram no ficheiro .xlsx
files = subdir('*00*.xlsx');
fileNames = {};
for i = 1:length(files)
   [path, name, ext] = fileparts(files(i).name);
   fileNames(i) = cellstr(name);
end
% Chamada das funcoes
time = createData(files, fileNames, 'A:A');
strain = createData(files, fileNames, 'C:C');
stress = createData(files, fileNames, 'E:E');
```

CreateData

```
function data = createData(f, n, col)
   for i = 1:length(f)
      data.(char(n(i))) = xlsread(f(i).name,1,col);
   end
end
```

ANNEX D: Modelling results

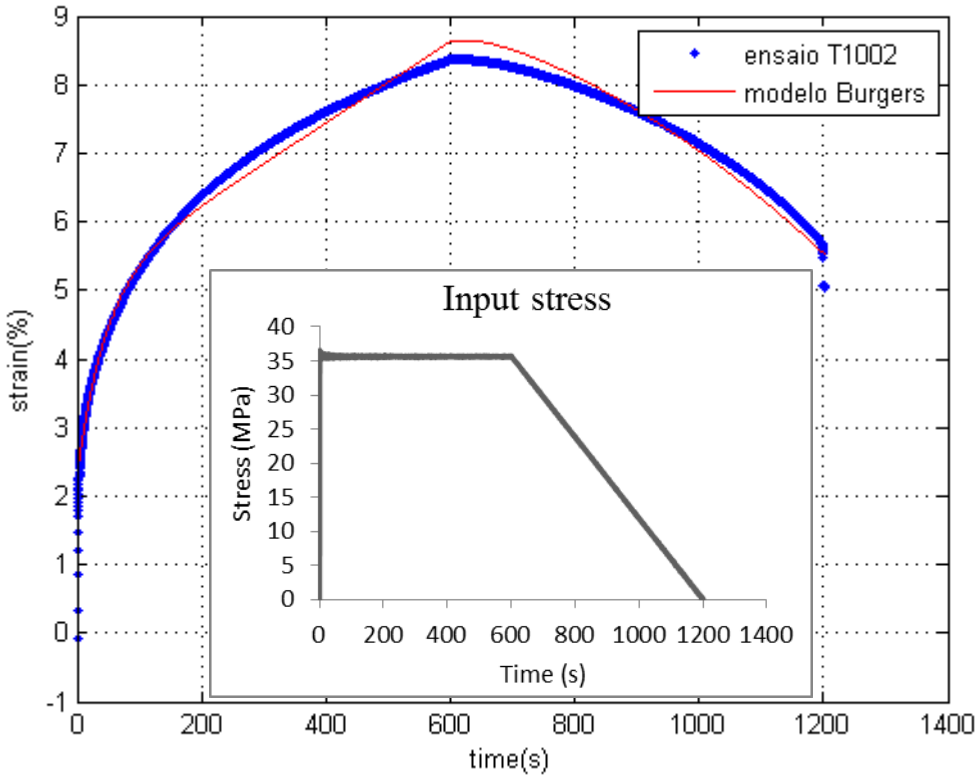

Figure 44 Result of the adjustment of the burgers equation to the results obtained in the creep test T1_002

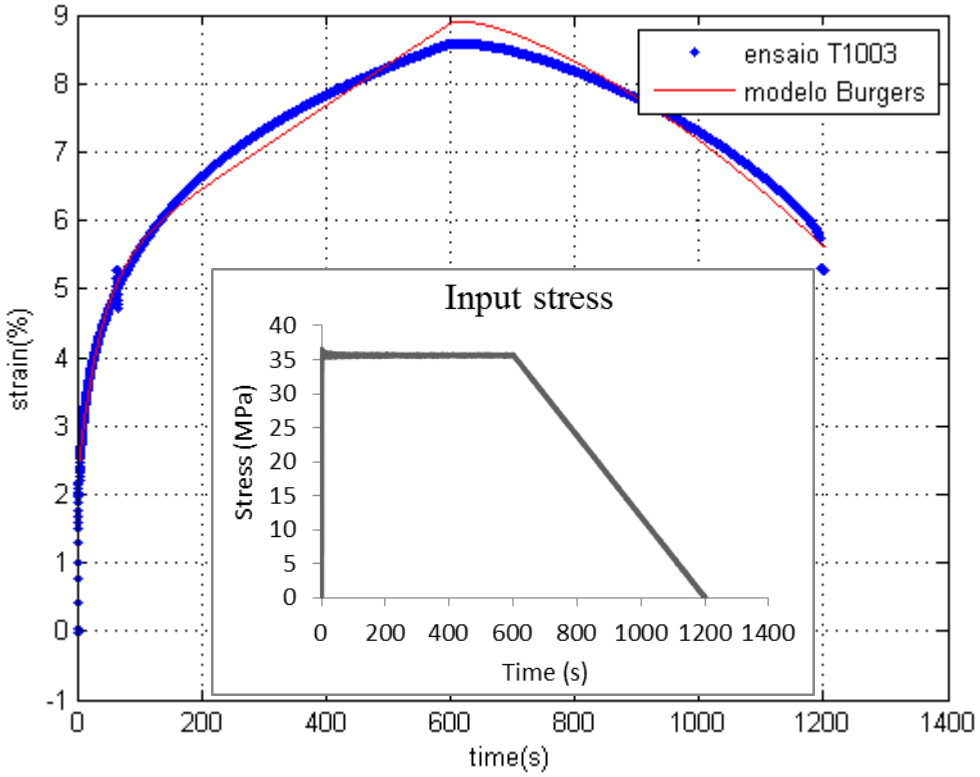

Figure 45 Result of the adjustment of the burgers equation to the results obtained in the creep test T1_003